A cytoplasmic Argonaute protein promotes the inheritance of RNAi

Fei Xu ╪, Xuezhu Feng ╪, Xiangyang Chen, Chenchun Weng, Qi Yan, Ting Xu, Minjie Hong, and Shouhong Guang *

School of Life Sciences, CAS Center for Excellence in Molecular Cell Science, University of Science and Technology of China, Hefei, Anhui 230027, P.R. China

╪These authors contributed equally to this work.

*To whom correspondence should be addressed. Tel.: +86 551 6360 7812, Fax: +86 551 6360 1443, E-mail: sguang@ustc.edu.cn

Running title: WAGO-4 mediates inheritance of RNAi

Keywords: Nrde, WAGO-4, inheritance, Argonaute, RNAi

Abstract:

RNAi-elicited gene silencing is heritable and can persist for multiple generations after its initial induction in *C. elegans*. However, the mechanism by which parental-acquired trait-specific information from RNAi is inherited by the progenies is not fully understood. Here, we identified a cytoplasmic Argonaute protein, WAGO-4, necessary for the inheritance of RNAi. WAGO-4 exhibits asymmetrical translocation to the germline during early embryogenesis, accumulates at the perinuclear foci in the germline, and is required for the inheritance of exogenous RNAi targeting both germline- and soma-expressed genes. WAGO-4 binds to 22G-RNA and its mRNA targets. Interestingly, WAGO-4-associated endogenous 22G-RNA targets the same cohort of germline genes as CSR-1 and similarly contains untemplated addition of uracil at the 3' ends. The poly(U) polymerase CDE-1 is required for the untemplated polyuridylation of WAGO-4-associated 22G-RNAs and inheritance of RNAi. Therefore, we conclude that cytoplasmic Argonaute proteins also promote the inheritance of RNAi in addition to the nuclear RNAi pathway.

Introduction:

RNAi-elicited gene silencing is heritable and can perpetuate for a number of generations in *C. elegans* (reviewed in (Heard and Martienssen, 2014; Miska and Ferguson-Smith, 2016; Rechavi and Lev, 2017)). Both exogenously derived siRNAs (exo-siRNAs) and endogenous small RNAs, such as endo-siRNAs and PIWI-interacting small RNAs (piRNAs), can trigger heritable RNAi. Transgenerational inheritance of RNAi allows organisms to remember their exposure to genome parasites, such as viruses and transposons, transmit the experience to descendants and promote evolutional advantages to enable selection for physiologically important traits. Although many lines of evidence have demonstrated that the RNAi machinery and small RNAs are involved in the initial establishment and ultimate maintenance of silencing, the precise nature of the trait-specific information that is transmitted from the parents to their progeny remains largely unclear (Buckley et al., 2012; Burton et al., 2017; Kalinava et al., 2017; Klosin et al., 2017; Lev et al., 2017; Marre et al., 2016; Spracklin et al., 2017; Weiser et al., 2017).

The mechanisms of transgenerational inheritance of RNAi are widely being investigated in *C. elegans*. The RNAi-mediated silencing effect can be transmitted *via* maternal or paternal gametes (Alcazar et al., 2008; Grishok et al., 2000) and its maintenance depends on the expression of the targeted genes in germline and post-transcriptional mechanisms (Minkina and Hunter, 2017). Chromatin-modifying enzymes and their associated factors, including HPL-2 (the chromatin-binding protein), SET-25 and SET-32 (the H3K9 methyltransferases), MES-2 (the H3K27 methyltransferase), and HDA-4 (a class II histone deacetylase), are engaged in the re-establishment and maintenance of transgenerational gene silencing (Ashe et al., 2012; Mao et al., 2015; Shirayama et al., 2012; Vastenhouw et al., 2006). In addition, the RNAi spreading defective factors RSD-2 and RSD-6 also promote genome silencing by maintaining transgenerational epigenetic inheritance of siRNA populations (Sakaguchi et al., 2014). The nuclear RNAi pathway plays essential roles in the inheritance of RNAi silencing (Ashe et al., 2012; Buckley et al., 2012; Burton et al.,

2011; Gu et al., 2012; Mao et al., 2015; Marre et al., 2016; Shirayama et al., 2012; Weiser et al., 2017). The germline-expressed nuclear Argonaute protein HRDE-1 (heritable RNAi deficient-1) may carry heritable small RNAs and engage in RNAi inheritance (Buckley et al., 2012). Interestingly, the nuclear RNAi pathway maintains siRNA expression in the progeny of dsRNA-treated animals (Burton et al., 2011).

Although many lines of evidence have demonstrated that the RNAi machinery and small RNAs are involved in the initial establishment and ultimate maintenance of silencing, the precise nature of the trait-specific information that is transferred from the parents to their progeny remains unknown. Both small RNAs and dsRNAs have been reported to transmit from the parents to the progeny in *C. elegans* (Rechavi and Lev, 2017). In addition, although it is widely known that the nuclear RNAi pathway plays important roles in RNAi inheritance, it is unclear whether and to what extent the cytoplasmic RNAi machinery contributes to this inheritance of RNAi (Spracklin et al., 2017).

To further understand the mechanisms of RNAi inheritance, we searched for factors required for silencing a germline-expressed *h2b::gfp* transgene in the progenies of animals exposed to exogenous *gfp* dsRNA. We isolated the cytoplasmic Argonaute protein WAGO-4. WAGO-4 is specifically required for the exogenous dsRNA-induced silencing of germline-expressed genes. WAGO-4 binds to germline-enriched 22G-RNAs containing the untemplated addition of uracil at their 3' ends, which depends on the poly(U) polymerase CDE-1. After fertilization, in the zygotes and early embryos, WAGO-4 exhibits asymmetrical translocation to the germline, suggesting that WAGO-4-involved cytoplasmic RNAi machinery may mediate the inheritance of RNAi by transmitting siRNA to the progeny. Therefore, we conclude that cytoplasmic RNAi machineries also contribute to the inheritance of RNAi, likely through cytoplasmic Argonaute proteins.

Results:

WAGO-4 is required for inheritance of RNAi.

DsRNA targeting *lin-15b* elicits a multivulva (Muv) phenotype in enhanced RNAi (*eri*) animals (but not in wild-type animals) through the nuclear RNAi defective (Nrde) pathway (Guang et al., 2008). However, the animals exhibit the Muv phenotype only in the F1 progeny but not at the parent animals, suggesting that the progenies have inherited a silencing signal. To look for genes involved in nuclear RNAi, we have previously tested a number of chromatin modification factors and Argonaute proteins by examining *lin-15*-RNAi induced Muv phenotype and *lir-1*-RNAi-induced larval arrest, but failed to identify any except for *nrde* and *mes-2* that were required to silence both operons (Mao et al., 2015). Interestingly, we found that an Argonaute gene, *wago-4*, was required for *lin-15*-RNAi-induced Muv phenotype in the F1 progeny but not for *lir-1*-RNAi-induced larval arrest at the parental generation, suggesting that WAGO-4 may act through the germline to mediate RNAi inheritance.

WAGO-4 belongs to the worm-specific clade Argonaute proteins with unknown functions (Yigit et al., 2006). To investigate its functions in RNAi inheritance, we acquired two deletion alleles, *tm1019* and *tm2401,* from the National BioResource Project (NBRP) (Figure S1A). We used dual sgRNA-mediated CRISPR/Cas9 technology to generate an additional allele, *ust42* (Figures S1A) (Chen et al., 2014). *tm1019* lacks the MID domain of Argonaute proteins; however, the remainder of the protein, including both the PAZ and the PIWI domains, is translated in frame. The alleles, *tm2401* and *ust42*, result in stop codons and are likely to be null alleles. *wago-4(ust42)* has been outcrossed twice and is used as the reference allele.

We confirmed that WAGO-4 was involved in dsRNA-induced gene silencing by feeding RNAi targeting a number of soma- and germline-expressed genes. RDE-4 is a dsRNA-binding protein indispensable for feeding RNAi targeting both soma- and germline-expressed genes, which served as a control for RNAi. *rde-4* mutants were resistant to the RNAi targeting of *pos-1, lir-1,* and *lin-15b* (Figure S1B). The somatic nuclear Argonaute protein NRDE-3 was required for dsRNA targeting of both *lir-1* and

lin-15b, the two examples used in nuclear RNAi analysis (Guang et al., 2008). *wago-4* was required for exogenous RNAi targeting *pos-1* in the germline or *lin-15b* which is predominantly expressed in the very early embryos, but not for RNAi targeting *lir-1* in the soma. Since *pos-1* was mainly silenced by RNAi in cytoplasm (Guang et al., 2008), this data suggested that WAGO-4 could conduct gene silencing in the cytoplasm in the germline.

We examined whether *wago-4* is required for the inheritance of RNAi. The germline-expressed nuclear Argonaute protein HRDE-1 is indispensable for RNAi inheritance (Buckley et al., 2012). We first used a germline-expressed *pie-1*$_p$*::gfp::h2b* (abbreviated as *h2b::gfp*) transgene as a reporter, which can inherit RNAi-induced gene silencing for multiple generations (Buckley et al., 2012). As reported, *hrde-1* was not required for exogenous *gfp* dsRNA to silence the *h2b::gfp* transgene at the parental generation but was required for the silencing in F1 animals (Figures 1A and S1C). Similarly, *wago-4* was not required for exogenous *gfp* dsRNA to silence the *h2b::gfp* transgene at the P0 generation, but was necessary to silence the *h2b::gfp* transgene in F1 progeny. For the somatic *sur-5::gfp* transgene, it was silenced by exogenous *gfp* dsRNA at both the P0 and F1 generations in wild-type animals (Figure 1B). However, in *wago-4* mutant animals, *sur-5::gfp* was silenced at P0 generation but desilenced at F1 generation, suggesting that the progeny failed to inherit the dsRNA-induced gene silencing effect. Interestingly, the fluorescence intensity of both *h2b::gfp* and *sur-5::gfp* transgenes did not reach the level of untreated animals in *wago-4* mutants, suggesting the presence of a weak RNAi inheritance even in the absence of *wago-4*. The *C. elegans'* genome encodes 27 Argonaute proteins, twelve of which belong to the WAGO clade including WAGO-4 (Yigit et al., 2006). We speculated that other WAGO proteins may function redundantly with WAGO-4 in mediating the inheritance of RNAi.

To further demonstrate that WAGO-4 promotes RNAi inheritance, we generated a single-copy WAGO-4 transgene *wago-4p::3xFLAG::GFP::WAGO-4* (abbreviated as *GFP::WAGO-4*) using MosSCI technology (Frokjaer-Jensen et al., 2014). This

transgene rescued *pos-1* and *mex-5* dsRNA-elicited embryonic lethality in *wago-4(ust42)* animals (Figures S1D and S1E), suggesting that the GFP::WAGO-4 represents the function and activity of endogenous WAGO-4 protein. *dpy-11* is an ortholog of human TMX4 and TMX1 genes and is required for body morphogenesis, which has been used for RNAi inheritance analysis (Minkina and Hunter, 2017). dsRNA targeting *dpy-11* in *eri-1* parental animals induced a dumpy phenotype in the F1 progeny in the absence of further RNAi, suggesting that the RNAi signal has been inherited (Figure 1C). While *rde-4* animals did not respond to feeding RNAi at all, the depletion of NRDE-3 or WAGO-4 both caused the loss of dumpy phenotype in F1 animals, suggesting that NRDE-3 and WAGO-4 were required for the inheritance of RNAi-targeting somatic genes. The introduction of GFP::WAGO-4 transgene rescued the inheritance defects in *wago-4* mutants.

Therefore, we concluded that *wago-4* promotes the inheritance of RNAi.

WAGO-4 is a germline-expressed Argonaute protein.

We examined the expression levels of *wago-4* mRNA at different developmental stages by downloading expression data from Wormbase (version WS260). *wago-4* mRNA was exclusively detected in the hermaphrodite germline but not in the soma (Figures 2A, S2A, and S2B). Additionally, GFP::WAGO-4 was expressed exclusively in the germline and all oocyte cells (including -1 oocyte) in gravid adults in hermaphrodites but not significantly expressed, if any, in the male germline (Figure S2A). In early embryos, WAGO-4 is expressed in the P1 and EMS cells at the two-cell and four-cell stages (Figure S2B). In late embryos, WAGO-4 was likely exclusively expressed in Z2/Z3 cells, which are the precursors of the germline. Interestingly, we observed that WAGO-4 accumulated at some distinct perinuclear foci (Figure 2B). Many RNA processing and regulating factors, including the RNAi machinery, are enriched in the perinuclear region and exhibit distinct foci, which are termed P-granules (Chen et al., 2016). A number of worm-specific Argonaute proteins, including WAGO-1 and CSR-1, accumulate in P-granules as well (Claycomb et al., 2009; Gu et al., 2009;

Tu et al., 2015; Wedeles et al., 2013). We crossed *GFP::WAGO-4* with a chromatin marker strain *H2B::mCherry* and the P-granule marker strain *mRuby::PGL-1*, respectively, and found that WAGO-4 partially co-localized with the P-granule marker PGL-1 but not the chromatin marker (Figures 2C).

We tested whether WAGO-4 was required for RNAi targeting germline-expressed genes by feeding L1 animals on dsRNA and harvested L4 animals of the same generation 48 hours later. The germline expressed mRNAs were examined by quantitative real-time PCR. Interestingly, although the PIWI domain of WAGO-4 lacks the DDH catalytic triad of amino acids considered necessary for Argonaute-based slicer activity (Yigit et al., 2006), WAGO-4 was required for the decrease of the targeted mRNAs by feeding RNAi (Figure 2D). This result suggested that either WAGO-4 still contains some slicer activity in the absence of DDH residues, or siRNA/WAGO-4 complex silences targeted mRNAs through additional mechanisms. Interestingly, *mex-5* and *pos-1* mRNAs were not fully desilenced in *wago-4* mutants, suggesting that other germline Argonaute proteins may function redundantly to silence germline genes.

WAGO-4 acts in multigenerational inheritance of RNAi.

To examine the roles of WAGO-4 in RNAi inheritance, we fed GFP::WAGO-4 animals with dsRNA targeting *oma-1* gene only at the P0 generation and isolated WAGO-4-bound siRNAs at later generations, followed by small RNA deep sequencing via a 5′-independent method. Sequencing analysis showed that WAGO-4 bound to *oma-1* siRNAs not only at the P0 and F1 generations, but also at the F3 generation (Figures 3A and 3B), suggesting that WAGO-4 could act in the multigenerational inheritance of RNAi.

Many RNAi inheritance mutants, including *hrde-1* animals, are defective in multigenerational inheritance of RNAi. These mutants exhibit a Mrt phenotype and gradually lose the fertility along generations (Buckley et al., 2012; Spracklin et al., 2017). We compared the Mrt phenotype of *hrde-1* and *wago-4* animals by examining

their brood size at 25℃ (Figure 3C). While *hrde-1* animals gradually lost the fecundity and achieved sterile at F3/F4 generations, *wago-4* animals exhibited a weaker Mrt phenotype and got sterile at the F8/F9 generations.

WAGO-4 and HRDE-1 act differently in promoting RNAi inheritance.

Both HRDE-1 and WAGO-4 are required for inheritance of RNAi, yet these proteins exhibit distinct subcellular locations and affinity to different cohorts of 22G-RNAs. We hypothesize that they function via different mechanisms or at distinct steps by depositing siRNAs from germline to zygote and/or re-establishing the silencing effects in the progeny.

To test this hypothesis, we treated *sur-5::gfp* parental animals with exogenous *gfp* dsRNA and examined *gfp* expression in F1 embryos and L4 larva without further feeding RNAi. RDE-1 is the Argonaute protein responsible for initiating RNAi in parental animals and is essential for feeding RNAi. *sur-5::gfp* was silenced in wild-type animals but not in *rde-1* mutants at the parental stage or F1 animals of embryos and L4 larva (Figure S3). In *hrde-1* and *nrde-1/2/4* mutants, *sur-5::gfp* was silenced in both parent animals and F1 embryos, indicating that the animals defective for nuclear RNAi are able to inherit *gfp* silencing signals (Burton et al., 2011; Weiser et al., 2017). However, during larval development, the heritable *gfp* silencing was relieved in *nrde-1/2/4* mutants but not in *hrde-1(-)* animals. *hrde-1(-)* mutants still exhibited an active somatic nuclear RNAi that conducted *gfp* silencing in the soma, further supporting that *hrde-1(-)* animals were able to inherit *gfp* silencing signals (Buckley et al., 2012).

We treated *wago-4(-);sur-5::gfp* animals with exogenous *gfp* dsRNA, examining *gfp* expression in F1 embryos, and quantifying the GFP levels using ImageJ (Figure 4A). In contrast to *hrde-1(-)* animals, in *wago-4* mutant, the *sur-5::gfp* was expressed in F1 embryos, although not to the levels of the *rde-1* mutant. Taken together, these results suggest that the HRDE-1-involved nuclear RNAi pathway is dispensable to directly transmit the trait-specific silencing information into the progeny. WAGO-4 is

likely engaged in transmitting 22G-RNAs from the parents to zygotes or at an earlier step than HRDE-1 to re-establish the silenced state in the progeny germline.

Previous genetic screening failed to identify WAGO proteins other than HRDE-1 that was required to mediate RNAi inheritance targeting *h2b::gfp* transgene (Buckley et al., 2012). The identification of WAGO-4 in RNAi inheritance suggested that these WAGO proteins should be re-investigated individually. We selected three other Argonaute proteins, in which C04F12.1 is closest to CSR-1 and WAGO-10 is closest to HRDE-1 based on sequence comparison (Gu et al., 2009). PPW-2 was closest to WAGO-4 and was required for the silencing of germline-expressed genes (data not shown). However, none of these three Argonaute proteins was required for the inheritance of RNAi targeting the *h2b::gfp* (Figure 4B). This data suggested that either WAGO-4 and the nuclear Argonaute HRDE-1 and NRDE-3 played special roles in RNAi inheritance, or *c04f12.1*, *wago-10*, and *ppw-2* may exhibit functional redundancy.

WAGO-4 binds 22G-RNAs.

To better understand the function of WAGO-4 in RNAi inheritance, we immunoprecipitated WAGO-4 before and after exogenous *lin-15b* dsRNA treatment (Figure S4A). Gravid P0 animals which contained a number of F1 embryos in the body were harvested. WAGO-4 associated mRNAs were purified and measured by quantitative real-time PCR analysis. WAGO-4 bound to *lin-15b* mRNA after *lin-15b* RNAi (Figure 5A). We then deep-sequenced WAGO-4-associated small RNAs in a 5'-phosphate-independent manner (Zhou et al., 2014). After immunoprecipitation of WAGO-4, small RNAs were isolated, pretreated with calf intestinal alkaline phosphatase to remove phosphate groups, treated with polynucleotide kinase to add a monophosphate group to the 5'-ends, and subjected to deep sequencing using the Illumina platform. Small RNA reads were aligned to the *C. elegans* transcriptome (WS243 assembly), and the number of small RNAs targeting each gene was counted. WAGO-4 preferentially binds to small RNAs antisense to *lin-15b* sequences in the presence of exogenous *lin-15b* dsRNA (Figure 5B). Although most of the reads cover

the region targeted by the *lin-15b* dsRNA, a portion of WAGO-4-associated siRNAs were derived from *lin-15b* sequences outside of the dsRNA region to which the animals were exposed (Figure 5C). In addition, most of the *lin-15b* siRNA reads are antisense to *lin-15b* mRNA. Although *lin-15b* and *lin-15a* are localized in the same operon and transcribed as a single pre-mRNA, they are spliced in the nucleus and exported individually into the cytoplasm. The siRNAs targeting *lin-15a* were not increased, which is consistent with the idea that RdRPs use mRNA in the cytoplasm, but not pre-mRNA in the nucleus, as templates to amplify secondary siRNAs (Pak and Fire, 2007). We further characterized WAGO-4-associated endogenous siRNAs. WAGO-4-associated endogenous siRNAs were 22 nt in length (Figure 5D), and the vast majority of the small RNAs started with G or GA at their 5' ends (Figures 5D and S4B), which are consistent with the properties of 22G-RNA. Together, these data suggested that WAGO-4-associated siRNAs were secondary siRNAs.

Approximately 93% of WAGO-4 bound 22G-RNAs target protein-coding genes (Figure 5E). We searched for WAGO-4 targets by selecting genes that had greater than 25 reads per million and identified 4,774 targeted genes (Table S1). We then compared WAGO-4-bound 22G-RNAs to other published small RNA categories (Figure 5F) (Gu et al., 2009; Tu et al., 2015; van Wolfswinkel et al., 2009). Consistent with its exclusive germline expression, WAGO-4 targets exhibited a pronounced overlap with *glp-4*-dependent genes. Interestingly, although WAGO-1, WAGO-4, and CSR-1 are all germline-expressed Argonaute proteins, WAGO-4 targets dramatically overlapped with those of CSR-1 but not WAGO-1, suggesting that WAGO-4 and CSR-1 may regulate the same cohorts of protein-coding genes in the germline. Noticeably, although *csr-1* mutant is homozygous lethal and exhibits chromosomal segregation defects (Claycomb et al., 2009; Gerson-Gurwitz et al., 2016), *wago-4* animals are viable and show no obvious growth defects at 20°C. *wago-4* mutants have similar brood size to that of wild-type animals at 20°C (Figure S4C). We quantified the mRNA levels of endogenous WAGO-4 22G-RNA targets by quantitative real time PCR, but failed to detect pronounced desilencing of the mRNA levels in *wago-4* mutants compared to wild-type

animals (Figure S4D). These data suggest that CSR-1 and WAGO-4 may function differently in gene regulation and animal development, although they largely bind to the same cohorts of germline-expressed 22G-RNAs.

WAGO-4-associated 22G-RNAs contain untemplated 3'-end polyuridylation.

We further analyzed the 3'-ends of WAGO-4-associated siRNAs and found that approximately 7.6% of the siRNAs contained an untemplated addition of uracil (Figure 6A). For reads longer than 23 nt, approximately 31% of them contained one extra U and 24.5% contained extra UU dinucleotides. We then examined the nucleotide distribution at each position of the small RNA reads (Figure S5A). Although the first two nucleotides exhibit a strong propensity towards the GA dinucleotide sequence and the nucleotides at position 3 to 5 have a modest enrichment of A, the four nucleotides (A, U, C, and G) are approximately equally distributed at each position in the middle of siRNAs in wild type animals. At the 3'-end, WAGO-4-associated 22G-RNAs exhibited a strong representation towards U.

CDE-1 is a polyuracil polymerase that adds untemplated uracils to CSR-1-associated 22G-RNAs and affects chromosome segregation (van Wolfswinkel et al., 2009). We examined whether CDE-1 is also involved in polyuridylating WAGO-4-associated 22G-RNAs by immunoprecipitating WAGO-4 from *cde-1(tm1021);3xFLAG::GFP::WAGO-4* animals and deep sequenced the associated small RNAs using a 5'-phosphate-independent method. The vast majority of WAGO-4-associated 22G-RNAs still targeted protein-coding genes (Figure S5B) and exhibited a tendency towards GA at 5'-end (Figure S5A), suggesting that CDE-1 is not essential for the biogenesis of WAGO-4-associated siRNAs. We analyzed the untemplated addition of uracil for all the small RNA reads or reads longer than 23 nt and found that the untemplated uracil addition was decreased in *cde-1* mutants. The percentage of one extra U was 7.6% in wild type and 2.5% in *cde-1* animals, and the percentage of two extra Us was 0.7% in wild type and 0.05% in *cde-1* animals (Figure 6B). For reads longer than 23 nt, the percentage of one extra U was 31% in wild type and 19% in *cde-*

1 animals, and the percentage of two extra Us was 24.5% in wild type and 5.8% in *cde-1* animals (Figure 6C).

Noticeably, although CDE-1 is not required for the association of WAGO-4 with 22G-RNAs targeting protein-coding genes, WAGO-4 bound approximately 24-fold more antisense ribosomal siRNAs (risiRNA) in *cde-1* mutants (31,409 reads per million in *cde-1* vs. 1,322 reads per million in wild-type animals) (Figure S5B) and 22-fold more small RNAs related to splicing leader sequences. We re-analyzed a published deep sequencing data set and identified similar increase of risiRNA (data not shown) (van Wolfswinkel et al., 2009). How CDE-1 is involved in risiRNA biogenesis remains mysterious (Zhou et al., 2017).

WAGO-4 and CSR-1 bind the same cohort of 22G-RNAs and are both polyuridylated at their 3'-ends by CDE-1. CDE-1-mediated uridylation is thought to destabilize CSR-1-bound 22G-RNAs (van Wolfswinkel et al., 2009). We re-analyzed published data of small RNAs associated with CSR-1 in *cde-1* and wild-type animals (van Wolfswinkel et al., 2009). CSR-1 targets with greater than 25 reads per million were selected. As reported, CSR-1 bound more 22G-RNAs in the *cde-1(tm1021)* mutant (Figure 6D). In contrast, WAGO-4 bound fewer 22G-RNAs targeting sites within protein coding genes in the *cde-1(tm1021)* mutant (Figure 6E). These data suggest that CDE-1-engaged polyuridylation likely stabilizes 22G-RNAs to bind WAGO-4 but destabilizes binding to CSR-1. We selected WAGO-4-associated 22G-RNAs that were decreased 2-fold and CSR-1-associated 22G-RNAs that were increased 2-fold in the *cde-1* mutant, and found that 1,344 genes were decreased in WAGO-4 binding but simultaneously increased in CSR-1 binding, implying a shift of 22G-RNA binding from WAGO-4 to CSR-1 in *cde-1* mutants (Figure 6F).

We then asked whether *cde-1* is required for the inheritance of RNAi. Similar to *hrde-1* and *wago-4*, *cde-1* was not required for exogenous dsRNA to silence the germline-expressed *h2b::gfp* transgene at the parental generation but was imperative

for silencing in F1 progeny (Figure S5C), which is consistent with a recent work (Spracklin et al., 2017). Taken together with the fact that CDE-1 stabilizes the binding of WAGO-4 to 22G-RNAs, we hypothesized that CDE-1 mediates RNAi inheritance by polyuridylating 22G-RNAs and promoting WAGO-4-engaged inheritance of RNAi.

WAGO-4 promotes the transmission of siRNAs for RNAi inheritance.

We further asked whether WAGO-4 is able to directly convey the silencing signal to progeny. WAGO-4 was expressed in both germline cells and oocytes (Figure 2B). Interestingly, in -1 to -3 oocytes, WAGO-4 still exhibited distinct foci, but mislocalized from the peri-nuclear region to the cytoplasm (Figure 7A). Early in the one-cell stage before chromosomal alignment, WAGO-4 is evenly distributed in the zygote without pronounced aggregation (Figures 7B). After chromosomal alignment in the one-cell stage, WAGO-4 began to accumulate in P-granule foci at the posterior ends (Figures 7B). The expression of WAGO-4 in -1 oocyte and the first-cell embryo suggested that WAGO-4 is able to carry siRNAs from the parent to progeny.

To further test whether WAGO-4 is involved in transmitting siRNAs, we used the subcellular localization of GFP::NRDE-3 as a reporter of siRNA abundance. NRDE-3 is a somatic Argonaute protein that localizes to the nucleus when it binds to siRNAs but accumulates in the cytoplasm in the absence of siRNA binding (Guang et al., 2008). In *eri-1* animals, NRDE-3 localizes in the cytoplasm, because *eri-1* is essential for the production of NRDE-3 siRNAs. In *eri-1;GFP::NRDE-3,* but not *eri-1;wago-4;GFP::NRDE-3,* animals, feeding RNAi targeting soma-expressed *dpy-11* and *lin-15b* genes elicited a cytoplasm-to-nucleus translocation of GFP::NRDE-3 in the F1 embryos (Figure 7C). Since the presence of mRNA templates were required for the amplification of secondary siRNAs, the siRNAs targeting soma-expressed genes (*dpy-11* and *lin-15b*) were not able to be amplified in the germline cells where the mRNA templates did not exist. The fact that the inheritance of RNAi targeting somatic genes depended on the germline-localized WAGO-4 proteins suggested that siRNAs were likely transmitted from the parental germline to the progeny embryos by WAGO-4. These siRNAs were

unable to be amplified in the germline but transported from the germline to the soma where they got amplified by RdRPs, induced nuclear accumulation of NRDE-3, and re-established silencing in the soma.

Taken together, these data suggested that WAGO-4 may directly promote the transmission of siRNAs from the parents to the progeny.

Discussion:

The inheritance of RNAi in *C. elegans* results from multiple steps, including initiation, transmission and re-establishment of silencing. Although the nuclear RNAi pathway and chromatin modification factors have been widely studied regarding their roles in the inheritance of RNAi, we demonstrated here that cytoplasmic Argonaute protein WAGO-4 and the polyuridylation polymerase CDE-1 may also play important roles in promoting inheritance of RNAi.

WAGO-4 promotes RNAi inheritance.

The nuclear RNAi pathway and chromatin modification factors play essential roles in transgenerational inheritance of RNAi (Heard and Martienssen, 2014; Rechavi and Lev, 2017). Recent work also suggests that RNAi spreading defective genes are involved in maintaining the inherited siRNAs (Rechavi and Lev, 2017). However, the precise nature of the trait-specific information that is deposited from the parents to their progeny remains unclear. Both small RNAs and dsRNA could be transmitted from the parents to the progeny to elicit gene silencing (Buckley et al., 2012; Marre et al., 2016). Here, we demonstrate that WAGO-4 promotes the inheritance of RNAi. WAGO-4 is localized to the perinuclear P-granule foci, suggesting that cytoplasmic RNAi machinery in addition to the nuclear RNAi pathway is involved in the inheritance of RNAi. The *C. elegans* genome encodes 27 Argonaute proteins, and many of these genes have unknown subcellular localizations and functions (Gu et al., 2009; Yigit et al., 2006). P-granule foci contain numerous RNA processing and regulating factors, including a few WAGOs (Chen et al., 2016). Whether these WAGOs act similarly to

WAGO-4 in mediating RNAi inheritance requires further investigation. Recently, Spracklin et al. reported a genetic screen that identified two P-granule-localized factors GLH-1/VASA and HRDE-2 engaged in transgenerational inheritance of gene silencing (Spracklin et al., 2017). This result further supported the idea that perinuclear P-granule machinery is indispensable for the inheritance of RNAi. However, it is unknown whether the P-granule structure itself is required for RNAi inheritance. It is possible that some of the P-granule factors, including WAGO-4, may translocate to other subcellular compartments at distinct developmental stages, or under certain environmental stimuli or genetic background, to mediate RNAi inheritance.

Previously it was reported that inherited small RNAs can spread from the germline to the soma and elicit gene silencing through the somatic nuclear RNAi pathway mediated by NRDE-3 (Burton et al., 2011). Given that WAGO-4 is expressed in both -1 oocyte and the one-cell embryo, it is very likely that WAGO-4 could carry 22G RNAs from the parental oocyte to the progeny. However, we could not exclude the possibility that dsRNAs are directly inherited to the progeny (Marre et al., 2016; Minkina and Hunter, 2017). To demonstrate that Argonaute proteins, including WAGO-4 and HRDE-1, directly transmit siRNAs from parent to progeny, we could isolate 1-cell F1 embryos, immunoprecipitate these Argonaute proteins, and test whether they bind to 22G-RNAs that were directly inherited from the parents in the absence of siRNA amplification step in F1 progeny. Additionally, we could perform single molecular in situ hybridization of siRNAs in very early embryos in wild type and *wago-4* mutants. However, both of these two methods are very technically challenging at current stage. In this work, using the subcellular localization of GFP::NRDE-3 as a siRNA sensor, we showed that a germline expressed Argonaute protein WAGO-4 is required for the production of siRNAs in the soma, suggesting that WAGO-4 is involved in the transmission of siRNAs from the parents to the progeny. A working model of RNAi inheritance was shown in Figure 7D.

HRDE-1 is a germline-expressed nuclear Argonaute protein that acts together with other NRDE proteins to promote RNAi inheritance (Buckley et al., 2012; Burton et al., 2011). In the *wago-4* mutant, in which HRDE presents, the inheritance of RNAi is compromised, suggesting that HRDE-1 is not sufficient to perform all the steps of initiation, transmission, and re-establishment of RNAi inheritance. Other Argonaute proteins, for example WAGO-4, may play indispensable roles in the inheritance of RNAi. Consistent with this idea, the F1 embryos of a silenced parent exhibit silencing in *hrde-1* mutants but desilencing in *wago-4* mutants.

Epigenetic changes can arise in the F1 embryos that are present inside the parents when the parental animals are exposed to environmental stimuli. These phenomena can be called as parental effects or intergenerational epigenetic inheritance (Anava et al., 2014; Heard and Martienssen, 2014; Houri-Zeevi and Rechavi, 2017). The epigenetic changes that are inherited and maintained for more than two or three generations are then called transgenerational inheritance. The RNAi-induced silencing status of the germline-expressed *h2b::gfp* transgene can be inherited for multiple generations and is widely used in transgenerational inheritance analysis (Buckley et al., 2012). In this work, we showed that *wago-4* was required for the inheritance of the silencing effect of the *h2b::gfp* transgene, suggesting that *wago-4* can be involved in the multigenerational inheritance of RNAi, as *hrde-1* does. This is further supported by the observation that the WAGO-4 binds to siRNAs in F3 generation after RNAi.

Stable maintenance of silencing requires an additional class of siRNAs that must be amplified in each generation. These siRNAs can be classified as secondary or tertiary siRNAs (Sapetschnig et al., 2015). It was shown that the production of tertiary siRNAs is part of a nuclear amplification pathway, which promotes germline integrity and possibly the inheritance of acquired physiological traits. Here, after feeding *lin-15b* dsRNA, most of the WAGO-4-associated 22G-RNAs locate very close to the dsRNA-targeted region of *lin-15b* RNAi, suggesting that these small RNAs are unlikely tertiary small RNAs. However, since we only deep sequenced WAGO-4-associated 22G-RNAs

from the P0 and F1 embryos, a more appropriate experiment should be to deep sequence WAGO-4-associated 22G-RNAs from later generations after RNAi.

Untemplated polyuridylation by CDE-1 is required for RNAi inheritance.

The polyU polymerase CDE-1 (also known as PUP-1 and CID-1) adds untemplated uracil to the 3' termini of RNAs in *C. elegans* (Kwak and Wickens, 2007; van Wolfswinkel et al., 2009). CDE-1 uridylates 22G-RNAs, which destabilizes the binding of 22G-RNAs to CSR-1 (van Wolfswinkel et al., 2009) but stabilizes the association between 22G-RNAs and WAGO-4. CSR-1 enhances gene expression when it binds to its favorite 22G-RNA (Gerson-Gurwitz et al., 2016). Disruption of *cde-1* increases these CSR-1 22G-RNAs and promotes gene expression. Taken together, we hypothesized that hyperactive CSR-1 and deficient WAGO-4 activity in *cde-1* mutants function together and mitigate the inheritance of RNAi. Noticeably, during the preparation of this manuscript, Spracklin et al. independently identified that CDE-1 is required for the inheritance of RNAi (Spracklin et al., 2017). The mechanism of CDE-1 to mediate RNAi inheritance is not fully understood. Here we showed that CDE-1 may regulate the 22G-RNAs that bind to WAGO-4. Yet compared with *wago-4* animals, *cde-1* mutants exhibited weaker GFP expression in the progeny, which might suggest the presence of a weak inheritance in *cde-1* mutants. Alternatively, this difference may also be due to the different efficiency of silencing re-establishment in these two mutated animals. A better experiment to compare the inheritance efficiency could be to measure the amounts of inherited siRNAs in the very early progeny embryos, in addition to quantifying the GFP intensity in larva.

Another important question is how Argonaute proteins selectively identify and bind to their siRNA ligands from a pool of short nuclear acids in the cell. In *Arabidopsis*, the 5' terminal nucleotide directs the sorting of small RNAs into different Argonaute complexes (Mi et al., 2008; Montgomery et al., 2008; Takeda et al., 2008). In *C. elegans*, although the 5'-triphosphorylated guanidine can provide a signal for secondary WAGO proteins, untemplated polyuridylation at the 3'-ends may function as an additional

sorting signal. There are a number of Argonaute proteins specifically expressed in the germline, including but not limiting to CSR-1, HRDE-1, WAGO-1, and WAGO-4. How each protein binds to its distinct cohort of 22G-RNAs and elicits different mechanisms to regulate gene expression remains a very intriguing question.

WAGO-4- and CSR-1-associated 22G-RNAs target the same cohort of germline-expressed protein-coding genes, suggesting that these two Argonaute proteins may compete for binding to 22G-RNAs. However, while *wago-4* promotes heritable RNAi silencing, the self-expressed endogenous mRNAs are protected by *csr-1* pathway (Shirayama et al., 2012). Additionally, *csr-1* mutant is homozygous lethal, while *wago-4* mutant did not exhibit fertility defects when grew at 20℃. It was shown that CSR-1 promotes gene expression upon binding to its favorable 22G-RNAs while silences some of its unfavorable targets (Claycomb et al., 2009; Gerson-Gurwitz et al., 2016). Therefore these two Argonaute proteins may use different mechanisms to elicit different outcomes in gene regulation. Disruption of the balance between these two Argonaute/siRNA complexes, such as in *cde-1* mutants, may cause serious growth defects.

Interestingly, although CDE-1 was not required for the association of WAGO-4 with 22G-RNAs targeting protein-coding genes, WAGO-4 bound significantly increased amount of risiRNAs and small RNAs related to splicing leader sequences in *cde-1* mutants. Currently the mechanism is unknown. One possibility is that CDE-1 may uridylate risiRNA and splicing leader sequences and subsequently induces the degradation of these sequences. Alternatively, CDE-1 may be involved in rRNA modification and/or processing, which is important for the maturation and homeostasis of rRNA. Erroneous rRNAs subsequently induces risiRNA generation, the mechanism of which also needs further investigation.

Asymmetrical distribution of siRNA.

Asymmetric cell divisions produce daughter cells of different sizes, molecular

content, and developmental potential, which promotes cell differentiation and specifies cell fate determination (Knoblich, 2001, 2008). In the early *C. elegans* embryo, a series of asymmetric divisions are crucial for establishing the three principal axes of the body plan and for segregating determinants that specify cell fates (Gonczy and Rose, 2005). The polarized distribution of PAR proteins plays essential roles in directing the unequal segregation of cell fate determinants to the anterior and posterior blastomeres. Recent genome-wide single-cell mRNA mapping technology has also started to elucidate the mRNA landscape at a single cell resolution and suggests unequal mRNA distribution to daughter cells (Osborne Nishimura et al., 2015; Tintori et al., 2016). Here, we demonstrate that the Argonaut protein WAGO-4 is unequally distributed to the posterior blastomere, possibly along with other P-granule components. WAGO-4-associated 22G-RNAs are consequently unequally distributed to daughter cells, which can subsequently modulate cell fate determination in corresponding cells. The asymmetric distribution of Argonaute proteins suggests that small RNAs may engage in tissue-specific gene regulation. Investigating how small RNAs are distributed to distinct cells by genome-wide single-cell mapping technology will help to illustrate the roles of RNAi machinery and small RNAs in embryonic development and cell fate determination (Gonczy and Rose, 2005; Osborne Nishimura et al., 2015; Tintori et al., 2016).

Materials and Methods:

Strains. Bristol strain N2 was used as the standard wild-type strain. All strains were incubated at 20 ℃. The following strains were used in this study: *hrde-1(tm1200)*, *wago-4(tm1019)*, *wago-4(tm2401)*, *wago-4(ust42)*, *eri-1(mg366)*, (YY380) *eri-1(mg366);rde-4(ne301)*, (YY189) *eri-1(mg366);nrde-3(gg066)*, (SHG503) *eri-1(mg366);wago-4(ust42)*, (YY513) *pkIs32[pie-1p::h2b::gfp]*, (YY528) *hrde-1(tm1200); pkIs32[pie-1p::h2b::gfp]*, (SHG480) *wago-4(tm1019); pkIs32[pie-1p::h2b::gfp]*, (SHG481) *wago-4(ust42); pkIs32[pie-1p::h2b::gfp]*, (SHG482) *wago-4(tm2401); pkIs32[pie-1p::h2b::gfp]*, (MH1870) *kuIs54[sur-5:::gfp]*, (YY518) *nrde-1(gg088);kuIS54[sur-5::gfp]*, (SHG039) *nrde-2(gg091);kuIS54[sur-5::gfp]*,

(YY521) *nrde-4(gg129); kuIS54[sur-5::gfp]*, (YY548) *hrde-1(tm1200);kuIs54[sur-5:::gfp]*, (SHG483) *rde-1(ne219); kuIs54[sur-5:::gfp]*, (SHG485) *wago-4(ust42); kuIs54[sur-5:::gfp]*, (SHG486) *wago-4(tm2401);kuIs54[sur-5:::gfp]*, (SHG487) *ustIs25[wago-4p::3xFLAG::GFP::wago-4]*, (SHG495) *cde-1(tm1021);ustIS25[wago-4p::3xFLAG::GFP::wago-4]*, (SHG366) *ustIs45[mex-5p::GFP::his-58::tbb-2utr]*, (SHG501) *hrde-1(tm1200);mex-5p::GFP::his-58::tbb-2utr*, (SHG502) *cde-1(tm1021);mex-5p::GFP::his-58::tbb-2utr*, (SHG341) *ustIs25[wago-4p::3xFLAG::GFP::wago-4];hjSi396[dpy-30p::mRuby::pgl-1]*, (SHG506) *ustIs25[wago-4p::3xFLAG::GFP::wago-4];ltIs37[(pAA64) pie-1p::mCherry::his-58 + unc-119(+)]*.

RNAi. RNAi experiments were conducted as described previously (Timmons et al., 2001). HT115 bacteria expressing the empty vector L4440 (a gift from A. Fire) were used as controls. Bacterial clones expressing dsRNA were obtained from the Ahringer RNAi library (Kamath et al., 2003) and were sequenced to verify their identities. *lin-15b* RNAi clones were described previously (Guang et al., 2008).

RNAi inheritance assay. Synchronized L1 animals of the indicated genotypes were exposed to bacteria expressing *gfp* dsRNA. F1 embryos were collected by hypochlorite/NaOH treatment and grown on HT115 control bacteria. GFP levels of animals in both parental generation and progeny were visualized and scored.

Images were collected on Leica DM2500 microscope. For the quantitation of GFP intensity, the average fluorescence intensities of L4 worms (0.5-second exposure) and embryos (1-second exposure) were analyzed using ImageJ (Borges and Martienssen, 2015). The background of each individual animal was subtracted using "the rolling ball radius" model of 3x3 pixels with the smoothing feature disabled. For subcellular localization analysis, approximately ten germlines were imaged and analyzed by ImageJ.

Images of co-localization analysis were collected on laica DM4 B microscope system with 100 1.4 NA APO oil-immersion objective under the control of Leica Application Suite X with a Laica DFC7000 D CCD camera (Laica corporation).

Mrt assay

Twenty larval stage L3 animals were singled to OP50 plates at each generation and cultured at 25℃. The average brood size at each generation was calculated.

Construction of plasmids and transgenic strains.

For 3xFLAG::GFP::WAGO-4, the 3xFLAG::GFP coding region was PCR amplified from plasmid pSG085 with the primers 5′-AGCTCTTCCTATGGACTACAAAGACCATGAC-3' and 5′-ATAGCTCCACCTCCACCTCCTTTGTATAGTTCATCCATGCC -3′. The predicted *wago-4* promoter was amplified from N2 genomic DNA with primers 5'-CGTGGATCCAGATATCCTGCAGGTTCGGTTACGCTCTCTCTCCAG -3′ and 5'-TGTAGTCCATAGGAAGAGCTGGCATCCTTCTC -3′. The *wago-4* coding region and predicted 3' UTR were then amplified by PCR from N2 genomic DNA with primers 5'- GGAGGTGGAGGAGGTGGAGCTATGCCAGCTCTTCCTCCAGTC-3' and 5'- GACTCACTAGTGGGCAGATCTCATCCCTGATGCCAAGCCGAC-3'. The plasmid pCFJ151 was digested with *Sbf*I and *Bgl*II. The three PCR fragments were cloned into linearized pCFJ151 with the homologous recombination kit (Vazyme C113-02) to generate a 3xFLAG::GFP::WAGO-4 fusion gene. The transgene was then integrated into the *C. elegans* genome using the mos1-mediated single copy insertion (MosSCI) method (Frokjaer-Jensen et al., 2014).

Dual sgRNA-directed *wago-4* deletion: Dual sgRNA-guided chromosome deletion was conducted as previously described (Chen et al., 2014). We manually searched for target sequences consisting of G(N)19NGG near the desired mutation sites in N2 genomic region. We replaced the *unc-119* target sequence in the pU6::unc-119 sgRNA vector with the desired target sequence using overlapped extension PCR with primer

pairs sgRNA-1F: 5'-GAAGATCCGCTCATGGTCAAGTTTTAGAGCTAGAAATAGCAAGTTA-3' and sgRNA-1R: 5'-CATGAGCGGATCTTCAAACATTTAGATTTGCAATTCAATTATATAG-3'; sgRNA-2F: 5'-GAATATTGCACCCGGTATTTGTTTTAGAGCTAGAAATAGCAAGTTA-3' and sgRNA-2R: 5'-CCGGGTGCAATATTCAAACATTTAGATTTGCAATTCAATTATATAG-3'; sgRNA-3F: 5'-GTTCAGAGAAGGCGCAGTAAGTTTTAGAGCTAGAAATAGCAAGTTA-3' and sgRNA-3R: 5'-GCGCCTTCTCTGAACAAACATTTAGATTTGCAATTCAATTATATAG-3'. Plasmid mixtures containing 50 ng/µl each of pU6::wago4 sgRNA1-3, 50 ng/µl Cas9 expression plasmid, 5 ng/µl pCFJ90 and 5 ng/µl pCFJ104 were co-injected into N2 animals. The deletion mutants were screened by PCR amplification.

Quantitative RT-PCR. RNAs were isolated from indicated animals using a dounce homogenizer (pestle B) in TRIzol solution followed by DNase I digestion (Qiagen), as described previously (Guang et al., 2008). cDNAs were generated from RNAs using the iScript cDNA Synthesis Kit (Bio-Rad) according to the vendor's protocol. qPCR was performed using a MyIQ2 machine (Bio-Rad) with iQ SYBR Green Supermix (Bio-Rad). The primers that were used in qRT-PCR are provided in Supplementary Table S2. *eft-3* mRNA was used as an internal control for sample normalization. Data analysis was performed using a ΔΔCT approach.

RNA immunoprecipitation (RIP). RIP experiments were performed as previously described with adult animals (Guang et al., 2008). Briefly, gravid adults were sonicated in sonication buffer (20 mM Tris-HCl [pH 7.5], 200 mM NaCl, 2.5 mM MgCl2, and 0.5% NP-40). The lysate was pre-cleared with protein G-agarose beads (Roche) and incubated with anti-FLAG M2 agarose beads (Sigma #A2220). The

beads were washed extensively and 3xFLAG::GFP::WAGO-4 and the associated RNAs were eluted with 100 μg/ml 3xFLAG peptide (Sigma). The eluates were incubated with TRIzol reagent followed by isopropanol precipitation. WAGO-4-bound RNAs were quantified by real-time PCR.

Isolation and sequencing of WAGO-4-associated small RNAs. WAGO-4-associated siRNAs were isolated from gravid adults as described above. The precipitated RNAs were treated with calf intestinal alkaline phosphatase (CIAP, Invitrogen), re-extracted with TRIzol, and treated with T4 polynucleotide kinase (T4 PNK, New England Biolabs) in the presence of 1 mM ATP (Zhou et al., 2014).

WAGO-4-bound siRNAs were subjected to deep sequencing using an Illumina platform, according to the manufacturer's instructions by the Beijing Genomics Institute (BGI Shenzhen). Small RNAs ranging from 18 to 30 nt were gel-purified and ligated to a 3' adaptor (5'-pUCGUAUGCCGUCUUCUGCUUGidT-3'; p, phosphate; idT, inverted deoxythymidine) and a 5' adaptor (5'-GUUCAGAGUUCUACAGUCCGACGAUC-3'). The ligation products were gel-purified, reverse transcribed, and amplified using Illumina's sRNA primer set (5'-CAAGCAGAAGACGGCATACGA-3'; 5'-AATGATACGGCGACCACCGA-3'). The samples were then sequenced using an Illumina Hiseq platform.

The Illumina-generated raw reads were first filtered to remove adaptors, low-quality tags and contaminants to obtain clean reads at BGI Shenzhen. Clean reads ranging from 18 to 30 nt were mapped to the unmasked *C. elegans* genome and the transcriptome assembly WS243, respectively, using Bowtie2 with default parameters (Langmead and Salzberg, 2012). The number of reads targeting each transcript was counted using custom Perl scripts and displayed by IGV (Thorvaldsdottir et al., 2013). The number of total reads mapped to the genome minus the number of total reads corresponding to sense rRNA transcripts (5S, 5.8S, 18S, and 26S) was used as the normalization number to exclude the possible degradation fragments of sense rRNAs.

Statistics: Bar graphs with error bars were presented with mean and s.d. All the experiments were conducted with independent *C. elegans* animals for indicated N times. Statistical analysis was performed with two-tailed Student's t-test.

Data availability: Argonaute-associated small RNAs from published data were re-analyzed. CSR-1 IP in wild type animals and in *cde-1* mutants, GSE17787 (van Wolfswinkel et al., 2009); WAGO-1 IP, SRR030711 (Gu et al., 2009); *glp-4(bn2)*, **GSM455394** (Gu et al., 2009).

All other data and materials are available upon request.

Author Contributions

F. X., X. F. and S. G. designed the experiments, F. X., X. F., X. C., C. W., Q. Y., T. X., and M. H. performed experiments. F. X., X. F. and S. G. analyzed the data. F. X., X. F. and S. G. wrote the manuscript. All authors have discussed the manuscript.

Additional Information

The authors declare no competing financial interests.

Acknowledgments

We are grateful to Dr. Scott Kennedy and members of the Guang lab for their comments. We are grateful to Dr. Ho Yi Mak, the International *C. elegans* Gene Knockout Consortium, and the National Bioresource Project for providing the strains. Some strains were provided by the CGC, which is funded by NIH Office of Research Infrastructure Programs (P40 OD010440). This work was supported by grants from the Chinese Ministry of Science and Technology (2017YFA0102903), the National Natural Science Foundation of China (Nos. 81501329, 31671346, and 91640110) and Anhui Natural Science Foundation (No. 1608085MC50).

References:

Alcazar, R.M., Lin, R., and Fire, A.Z. (2008). Transmission dynamics of heritable silencing induced by double-stranded RNA in *Caenorhabditis elegans*. Genetics *180*, 1275-1288.

Anava, S., Posner, R., and Rechavi, O. (2014). The soft genome. Worm *3*, e989798.

Ashe, A., Sapetschnig, A., Weick, E.M., Mitchell, J., Bagijn, M.P., Cording, A.C., Doebley, A.L., Goldstein, L.D., Lehrbach, N.J., Le Pen, J.*, et al.* (2012). piRNAs Can Trigger a Multigenerational Epigenetic Memory in the Germline of *C. elegans*. Cell *150*, 88-99.

Borges, F., and Martienssen, R.A. (2015). The expanding world of small RNAs in plants. Nature reviews Molecular cell biology *16*, 727-741.

Buckley, B.A., Burkhart, K.B., Gu, S.G., Spracklin, G., Kershner, A., Fritz, H., Kimble, J., Fire, A., and Kennedy, S. (2012). A nuclear Argonaute promotes multigenerational epigenetic inheritance and germline immortality. Nature *489*, 447-451.

Burton, N.O., Burkhart, K.B., and Kennedy, S. (2011). Nuclear RNAi maintains heritable gene silencing in *Caenorhabditis elegans*. Proceedings of the National Academy of Sciences of the United States of America *108*, 19683-19688.

Burton, N.O., Furuta, T., Webster, A.K., Kaplan, R.E., Baugh, L.R., Arur, S., and Horvitz, H.R. (2017). Insulin-like signalling to the maternal germline controls progeny response to osmotic stress. Nature cell biology *19*, 252-257.

Chen, J.X., Cipriani, P.G., Mecenas, D., Polanowska, J., Piano, F., Gunsalus, K.C., and Selbach, M. (2016). In Vivo Interaction Proteomics in *Caenorhabditis elegans* Embryos Provides New Insights into P Granule Dynamics. Mol Cell Proteomics *15*, 1642-1657.

Chen, X., Xu, F., Zhu, C., Ji, J., Zhou, X., Feng, X., and Guang, S. (2014). Dual sgRNA-directed gene knockout using CRISPR/Cas9 technology in *Caenorhabditis elegans*. Sci Rep *4*, 7581.

Claycomb, J.M., Batista, P.J., Pang, K.M., Gu, W., Vasale, J.J., van Wolfswinkel, J.C., Chaves, D.A., Shirayama, M., Mitani, S., Ketting, R.F.*, et al.* (2009). The Argonaute CSR-1 and its 22G-RNA cofactors are required for holocentric chromosome segregation. Cell *139*, 123-134.

Frokjaer-Jensen, C., Davis, M.W., Sarov, M., Taylor, J., Flibotte, S., LaBella, M., Pozniakovsky, A., Moerman, D.G., and Jorgensen, E.M. (2014). Random and targeted transgene insertion in Caenorhabditis elegans using a modified Mos1 transposon. Nature methods *11*, 529-534.

Gerson-Gurwitz, A., Wang, S., Sathe, S., Green, R., Yeo, G.W., Oegema, K., and Desai, A. (2016). A Small RNA-Catalytic Argonaute Pathway Tunes Germline Transcript Levels to Ensure Embryonic Divisions. Cell *165*, 396-409.

Gonczy, P., and Rose, L.S. (2005). Asymmetric cell division and axis formation in the embryo. WormBook : the online review of C elegans biology, 1-20.

Grishok, A., Tabara, H., and Mello, C.C. (2000). Genetic requirements for inheritance of RNAi in *C. elegans*. Science *287*, 2494-2497.

Gu, S.G., Pak, J., Guang, S., Maniar, J.M., Kennedy, S., and Fire, A. (2012). Amplification of siRNA in *Caenorhabditis elegans* generates a transgenerational sequence-targeted histone H3 lysine 9 methylation footprint. Nature genetics *44*, 157-164.

Gu, W., Shirayama, M., Conte, D., Jr., Vasale, J., Batista, P.J., Claycomb, J.M., Moresco, J.J., Youngman, E.M., Keys, J., Stoltz, M.J.*, et al.* (2009). Distinct argonaute-mediated 22G-RNA pathways direct genome surveillance in the *C. elegans* germline. Molecular cell *36*, 231-244.

Guang, S., Bochner, A.F., Pavelec, D.M., Burkhart, K.B., Harding, S., Lachowiec, J., and Kennedy, S. (2008).

An Argonaute transports siRNAs from the cytoplasm to the nucleus. Science *321*, 537-541.
Heard, E., and Martienssen, R.A. (2014). Transgenerational epigenetic inheritance: myths and mechanisms. Cell *157*, 95-109.
Houri-Zeevi, L., and Rechavi, O. (2017). A Matter of Time: Small RNAs Regulate the Duration of Epigenetic Inheritance. Trends in genetics : TIG *33*, 46-57.
Kalinava, N., Ni, J.Z., Peterman, K., Chen, E., and Gu, S.G. (2017). Decoupling the downstream effects of germline nuclear RNAi reveals that H3K9me3 is dispensable for heritable RNAi and the maintenance of endogenous siRNA-mediated transcriptional silencing in Caenorhabditis elegans. Epigenetics & chromatin *10*, 6.
Kamath, R.S., Fraser, A.G., Dong, Y., Poulin, G., Durbin, R., Gotta, M., Kanapin, A., Le Bot, N., Moreno, S., Sohrmann, M.*, et al.* (2003). Systematic functional analysis of the Caenorhabditis elegans genome using RNAi. Nature *421*, 231-237.
Klosin, A., Casas, E., Hidalgo-Carcedo, C., Vavouri, T., and Lehner, B. (2017). Transgenerational transmission of environmental information in C. elegans. Science *356*, 320-323.
Knoblich, J.A. (2001). Asymmetric cell division during animal development. Nature reviews Molecular cell biology *2*, 11-20.
Knoblich, J.A. (2008). Mechanisms of asymmetric stem cell division. Cell *132*, 583-597.
Kwak, J.E., and Wickens, M. (2007). A family of poly(U) polymerases. Rna *13*, 860-867.
Langmead, B., and Salzberg, S.L. (2012). Fast gapped-read alignment with Bowtie 2. Nature methods *9*, 357-359.
Lev, I., Seroussi, U., Gingold, H., Bril, R., Anava, S., and Rechavi, O. (2017). MET-2-Dependent H3K9 Methylation Suppresses Transgenerational Small RNA Inheritance. Current biology : CB *27*, 1138-1147.
Mao, H., Zhu, C., Zong, D., Weng, C., Yang, X., Huang, H., Liu, D., Feng, X., and Guang, S. (2015). The Nrde Pathway Mediates Small-RNA-Directed Histone H3 Lysine 27 Trimethylation in *Caenorhabditis elegans*. Current biology : CB *25*, 2398-2403.
Marre, J., Traver, E.C., and Jose, A.M. (2016). Extracellular RNA is transported from one generation to the next in *Caenorhabditis elegans*. Proceedings of the National Academy of Sciences of the United States of America *113*, 12496-12501.
Mi, S., Cai, T., Hu, Y., Chen, Y., Hodges, E., Ni, F., Wu, L., Li, S., Zhou, H., Long, C.*, et al.* (2008). Sorting of small RNAs into Arabidopsis argonaute complexes is directed by the 5' terminal nucleotide. Cell *133*, 116-127.
Minkina, O., and Hunter, C.P. (2017). Stable Heritable Germline Silencing Directs Somatic Silencing at an Endogenous Locus. Molecular cell *65*, 659-670 e655.
Miska, E.A., and Ferguson-Smith, A.C. (2016). Transgenerational inheritance: Models and mechanisms of non-DNA sequence-based inheritance. Science *354*, 59-63.
Montgomery, T.A., Howell, M.D., Cuperus, J.T., Li, D., Hansen, J.E., Alexander, A.L., Chapman, E.J., Fahlgren, N., Allen, E., and Carrington, J.C. (2008). Specificity of ARGONAUTE7-miR390 interaction and dual functionality in TAS3 trans-acting siRNA formation. Cell *133*, 128-141.
Osborne Nishimura, E., Zhang, J.C., Werts, A.D., Goldstein, B., and Lieb, J.D. (2015). Asymmetric transcript discovery by RNA-seq in *C. elegans* blastomeres identifies neg-1, a gene important for anterior morphogenesis. PLoS genetics *11*, e1005117.
Pak, J., and Fire, A. (2007). Distinct populations of primary and secondary effectors during RNAi in *C. elegans*. Science *315*, 241-244.
Rechavi, O., and Lev, I. (2017). Principles of Transgenerational Small RNA Inheritance in Caenorhabditis

elegans. Current biology : CB *27*, R720-R730.
Sakaguchi, A., Sarkies, P., Simon, M., Doebley, A.L., Goldstein, L.D., Hedges, A., Ikegami, K., Alvares, S.M., Yang, L., LaRocque, J.R.*, et al.* (2014). *Caenorhabditis elegans* RSD-2 and RSD-6 promote germ cell immortality by maintaining small interfering RNA populations. Proceedings of the National Academy of Sciences of the United States of America *111*, E4323-4331.
Sapetschnig, A., Sarkies, P., Lehrbach, N.J., and Miska, E.A. (2015). Tertiary siRNAs mediate paramutation in C. elegans. PLoS genetics *11*, e1005078.
Shirayama, M., Seth, M., Lee, H.C., Gu, W., Ishidate, T., Conte, D., Jr., and Mello, C.C. (2012). piRNAs initiate an epigenetic memory of nonself RNA in the *C. elegans* germline. Cell *150*, 65-77.
Spracklin, G., Fields, B., Wan, G., Vijayendran, D., Wallig, A., Shukla, A., and Kennedy, S. (2017). Identification and Characterization of Caenorhabditis elegans RNAi Inheritance Machinery. Genetics.
Takeda, A., Iwasaki, S., Watanabe, T., Utsumi, M., and Watanabe, Y. (2008). The mechanism selecting the guide strand from small RNA duplexes is different among argonaute proteins. Plant & cell physiology *49*, 493-500.
Thorvaldsdottir, H., Robinson, J.T., and Mesirov, J.P. (2013). Integrative Genomics Viewer (IGV): high-performance genomics data visualization and exploration. Briefings in bioinformatics *14*, 178-192.
Timmons, L., Court, D.L., and Fire, A. (2001). Ingestion of bacterially expressed dsRNAs can produce specific and potent genetic interference in *Caenorhabditis elegans*. Gene *263*, 103-112.
Tintori, S.C., Osborne Nishimura, E., Golden, P., Lieb, J.D., and Goldstein, B. (2016). A Transcriptional Lineage of the Early *C. elegans* Embryo. Developmental cell *38*, 430-444.
Tu, S., Wu, M.Z., Wang, J., Cutter, A.D., Weng, Z., and Claycomb, J.M. (2015). Comparative functional characterization of the CSR-1 22G-RNA pathway in *Caenorhabditis nematodes*. Nucleic acids research *43*, 208-224.
van Wolfswinkel, J.C., Claycomb, J.M., Batista, P.J., Mello, C.C., Berezikov, E., and Ketting, R.F. (2009). CDE-1 affects chromosome segregation through uridylation of CSR-1-bound siRNAs. Cell *139*, 135-148.
Vastenhouw, N.L., Brunschwig, K., Okihara, K.L., Muller, F., Tijsterman, M., and Plasterk, R.H. (2006). Gene expression: long-term gene silencing by RNAi. Nature *442*, 882.
Wedeles, C.J., Wu, M.Z., and Claycomb, J.M. (2013). Protection of germline gene expression by the *C. elegans* Argonaute CSR-1. Developmental cell *27*, 664-671.
Weiser, N.E., Yang, D.X., Feng, S., Kalinava, N., Brown, K.C., Khanikar, J., Freeberg, M.A., Snyder, M.J., Csankovszki, G., Chan, R.C.*, et al.* (2017). MORC-1 Integrates Nuclear RNAi and Transgenerational Chromatin Architecture to Promote Germline Immortality. Developmental cell *41*, 408-423 e407.
Yigit, E., Batista, P.J., Bei, Y., Pang, K.M., Chen, C.C., Tolia, N.H., Joshua-Tor, L., Mitani, S., Simard, M.J., and Mello, C.C. (2006). Analysis of the *C. elegans* Argonaute family reveals that distinct Argonautes act sequentially during RNAi. Cell *127*, 747-757.
Zhou, X., Feng, X., Mao, H., Li, M., Xu, F., Hu, K., and Guang, S. (2017). RdRP-synthesized antisense ribosomal siRNAs silence pre-rRNA via the nuclear RNAi pathway. Nature structural & molecular biology.
Zhou, X., Xu, F., Mao, H., Ji, J., Yin, M., Feng, X., and Guang, S. (2014). Nuclear RNAi contributes to the silencing of off-target genes and repetitive sequences in *Caenorhabditis elegans*. Genetics *197*, 121-132.

Figure Legends:

Figure 1: WAGO-4 is required for the inheritance of RNAi. (a) *pie-1$_p$::gfp::h2b* transgenic animals were exposed to bacteria expressing *gfp* dsRNA. F1 embryos were isolated and grown on HT115 control bacteria in the absence of further *gfp* dsRNA treatment. GFP expression in oocytes were imaged. Percentage of F1 animals expressing GFP was counted. (b) Animals expressing somatic *sur-5::gfp* transgene were treated with *gfp* dsRNA. F1 embryos were isolated and grown on HT115 control bacteria. GFP expression of the whole animals were imaged. The *gfp* levels were scored. (c) Rescue assay of the GFP::WAGO-4 transgene. The indicated animals were treated with *dpy-11* dsRNA and F1 animals were transferred to HT115 control bacteria (upper panel). The levels of dumpyness were scored (lower panel). ***p<0.001.

Figure 2: WAGO-4 is a germline-expressed Argonaute protein. (a) The expression levels of *wago-4* mRNA at different developmental stages. Data were downloaded from Wormbase (version WS260). EE, early embryos; LE, late embryos; YA, young adults. (b) Images of the germline of the GFP::WAGO-4 strain. (c) Pachytene germ cells of GFP::WAGO-4 and the chromatin marker H2B::mCherry and p-granule marker mRuby::PGL-1 were imaged. (d) Wild-type and *wago-4(-)* animals were treated with indicated dsRNAs. Total RNAs were isolated at L4 stage of P0 generation and the indicated mRNAs were quantified by real-time PCR. mean ± s.d. n=3. *p<0.05, **p<0.01, ***p<0.001, ns, not significant.

Figure 3. WAGO-4 acts in multigenerational inheritance of RNAi. (a) WAGO-4-associated small RNAs targeting *oma-1* locus is shown. Red ticks are sense reads to *oma-1* sequence, blue ticks are antisense reads. GFP::WAGO-4 animals were first treated with *oma-1* dsRNA at P0 generation and then fed on control bacteria in the absence of *oma-1* dsRNA in subsequent generations. GFP::WAGO-4 was immunoprecipitated from young adult animals and the associated small RNAs were deep sequenced. Animals fed on control RNAi bacteria were set as control. (b) Normalized number of antisense reads of indicated animals. (c) Brood size of indicated

animals by Mrt assay at 25℃. N=20, mean±s.d..

Figure 4: WAGO-4 and HRDE-1 act differently to promote RNAi inheritance. (a) Images of indicated animals after *gfp* RNAi. *sur-5::gfp* animals were fed on *gfp* dsRNA and the F1 embryos were incubated on HT115 control bacteria. Upper panel: fluorescent images of indicated animals after *gfp* RNAi. Bottom panel: GFP intensity levels of the indicated animals were measured by ImageJ. The number of animals assayed is indicated. *p<0.05, **p<0.01, ***p<0.001, ns, not significant. (b) Images of germline cells of indicated animals. *gfp::h2b* animals were fed on *gfp* dsRNA and the F1 embryos were incubated on HT115 control bacteria. The *gfp* levels were scored and shown in the lower panel.

Figure 5: WAGO-4 binds to 22G-RNA. (a) WAGO-4 was immunoprecipitated at young gravid stage after *lin-15b* RNAi, and the associated RNAs were quantified by real-time PCR. mean ±s.d. n=3. (b) WAGO-4 was immunoprecipitated at young gravid stage, and the associated siRNAs were deep sequenced. The number of reads with or without *lin-15b* RNAi were normalized and then compared. (c) Reads targeting *lin-15b/a* genomic loci were plotted. Yellow box indicates the dsRNA-targeted region. (d) The length distribution and first nucleotides of WAGO-4-associated siRNAs were analyzed. (e) The WAGO-4 22G-RNA targets were grouped into different categories. (f) The WAGO-4 22G-RNA targets were compared with other known small RNA categories.

Figure 6: CDE-1 polyuridylates WAGO-4 22G-RNAs and promotes RNAi inheritance. (a) The untemplated 3'-end addition of nucleotides of WAGO-4-bound 22G-RNAs was analyzed. Left, total reads; right, reads longer than 23 nt. (b) Comparison of the untemplated addition of nucleotides of WAGO-4 22G-RNAs in wild-type animals and *cde-1* mutants. The insert plot is a zoom in of the main figure. (c) Comparison of the untemplated addition of nucleotides of WAGO-4 22G-RNAs for reads longer than 23 nt. (d) Analysis of CSR-1 22G-RNAs in *cde-1* mutants. (e)

Analysis of WAGO-4 22G-RNAs in *cde-1* mutants. (f) Comparison of WAGO-4 and CSR-1 22G-RNAs in *cde-1* mutants. ***p<0.001.

Figure 7: WAGO-4 promotes transmission of siRNAs from parents to progeny. (a, b) Images of oocytes and early embryos of the *GFP::WAGO-4;mCherry::H2B* strain. (c) Images of F1 embryos of the indicated animals after feeding RNAi targeting L4 animals for 24 hours. The percentage of nuclear localized NRDE-3 in F1 embryos were indicated. The number of scored animals were indicated in the parentheses. N, nucleus. (d) A working model of the WAGO-4-mediated inheritance of RNAi. WAGO-4 is involved in transmitting the siRNA pool along generations as well as conducting gene silencing in the germline. Inherited small RNAs targeting soma-expressed genes are translocated to the soma of the progeny to get amplified and silence somatic gene expression. siRNAs targeting germline-expressed genes silence gene expression in the germline of the progeny. Meanwhile, the germline-targeting siRNAs can also be amplified by RdRPs and transmitted to next progeny by WAGO-4, which therefore maintain the RNAi silencing status for multiple generations.

Figure 1

A

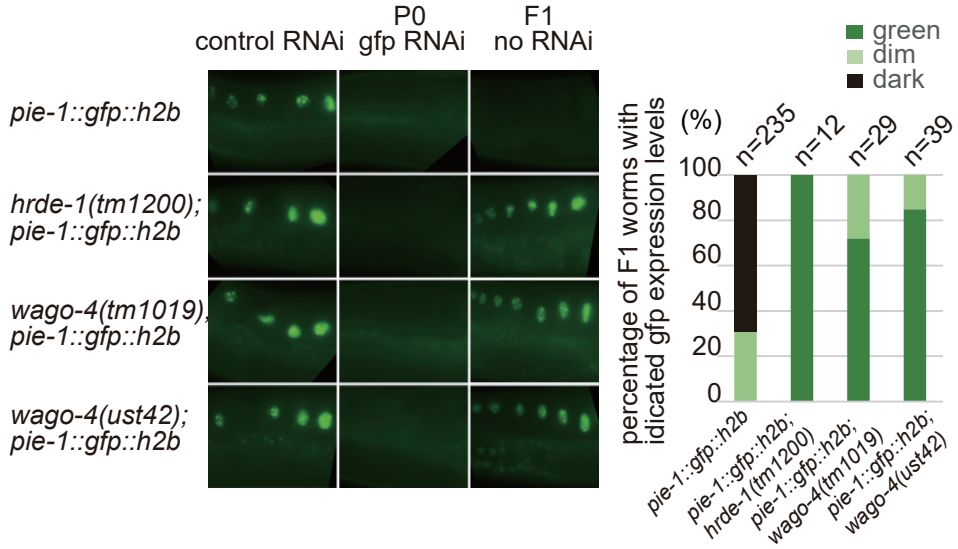
control RNAi
P0 gfp RNAi
F1 no RNAi
pie-1::gfp::h2b
hrde-1(tm1200); pie-1::gfp::h2b
wago-4(tm1019); pie-1::gfp::h2b
wago-4(ust42); pie-1::gfp::h2b
green
dim
dark
percentage of F1 worms with idicated gfp expression levels
(%)
100
80
60
40
20
0
n=235
n=12
n=29
n=39
pie-1::gfp::h2b
pie-1::gfp::h2b; hrde-1(tm1200)
pie-1::gfp::h2b; wago-4(tm1019)
pie-1::gfp::h2b; wago-4(ust42)

B

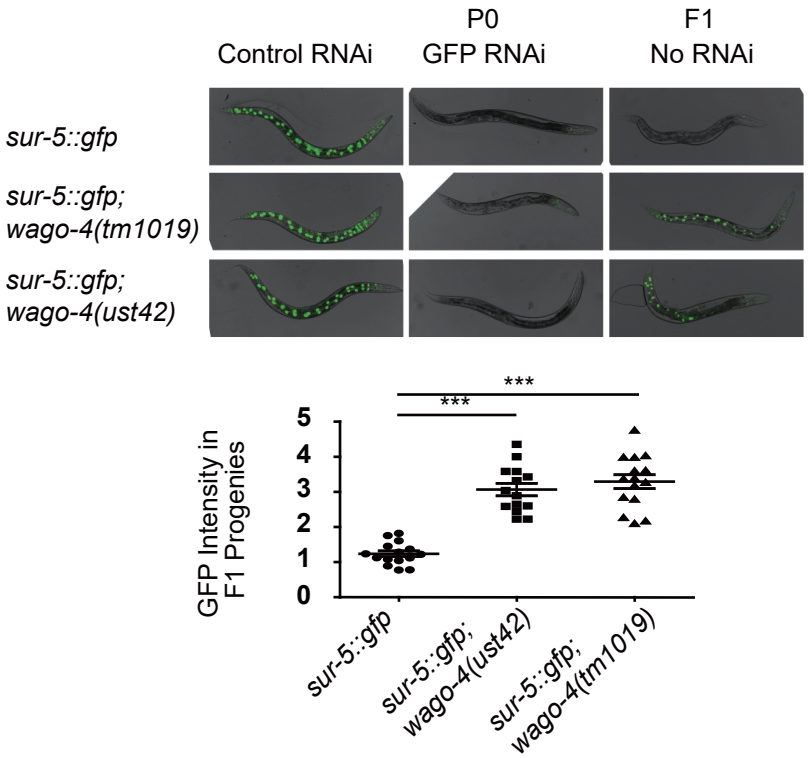
Control RNAi
P0 GFP RNAi
F1 No RNAi
sur-5::gfp
sur-5::gfp; wago-4(tm1019)
sur-5::gfp; wago-4(ust42)
GFP Intensity in F1 Progenies
5
4
3
2
1
0
***
***
sur-5::gfp
sur-5::gfp; wago-4(ust42)
sur-5::gfp; wago-4(tm1019)

C

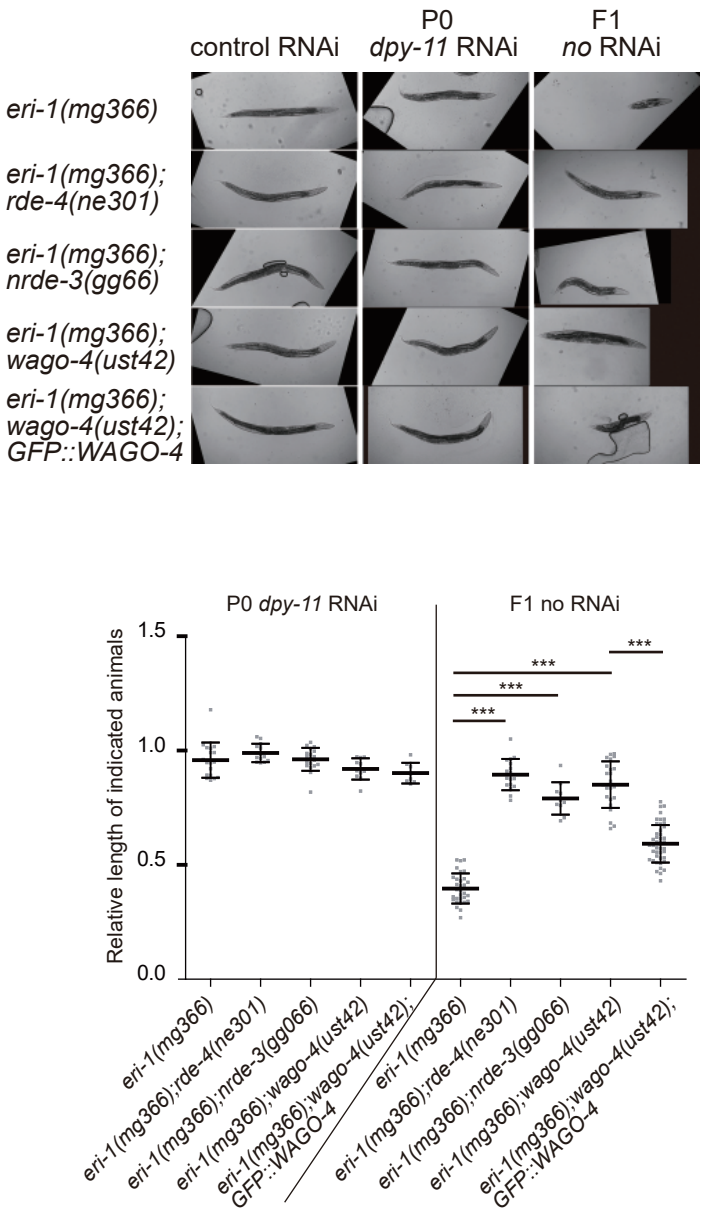
control RNAi
P0 dpy-11 RNAi
F1 no RNAi
eri-1(mg366)
eri-1(mg366); rde-4(ne301)
eri-1(mg366); nrde-3(gg66)
eri-1(mg366); wago-4(ust42)
eri-1(mg366); wago-4(ust42); GFP::WAGO-4
P0 dpy-11 RNAi
F1 no RNAi
Relative length of indicated animals
1.5
1.0
0.5
0.0
***
***
***
***
eri-1(mg366)
eri-1(mg366);rde-4(ne301)
eri-1(mg366);nrde-3(gg066)
eri-1(mg366);wago-4(ust42)
eri-1(mg366);wago-4(ust42); GFP::WAGO-4

Figure 2

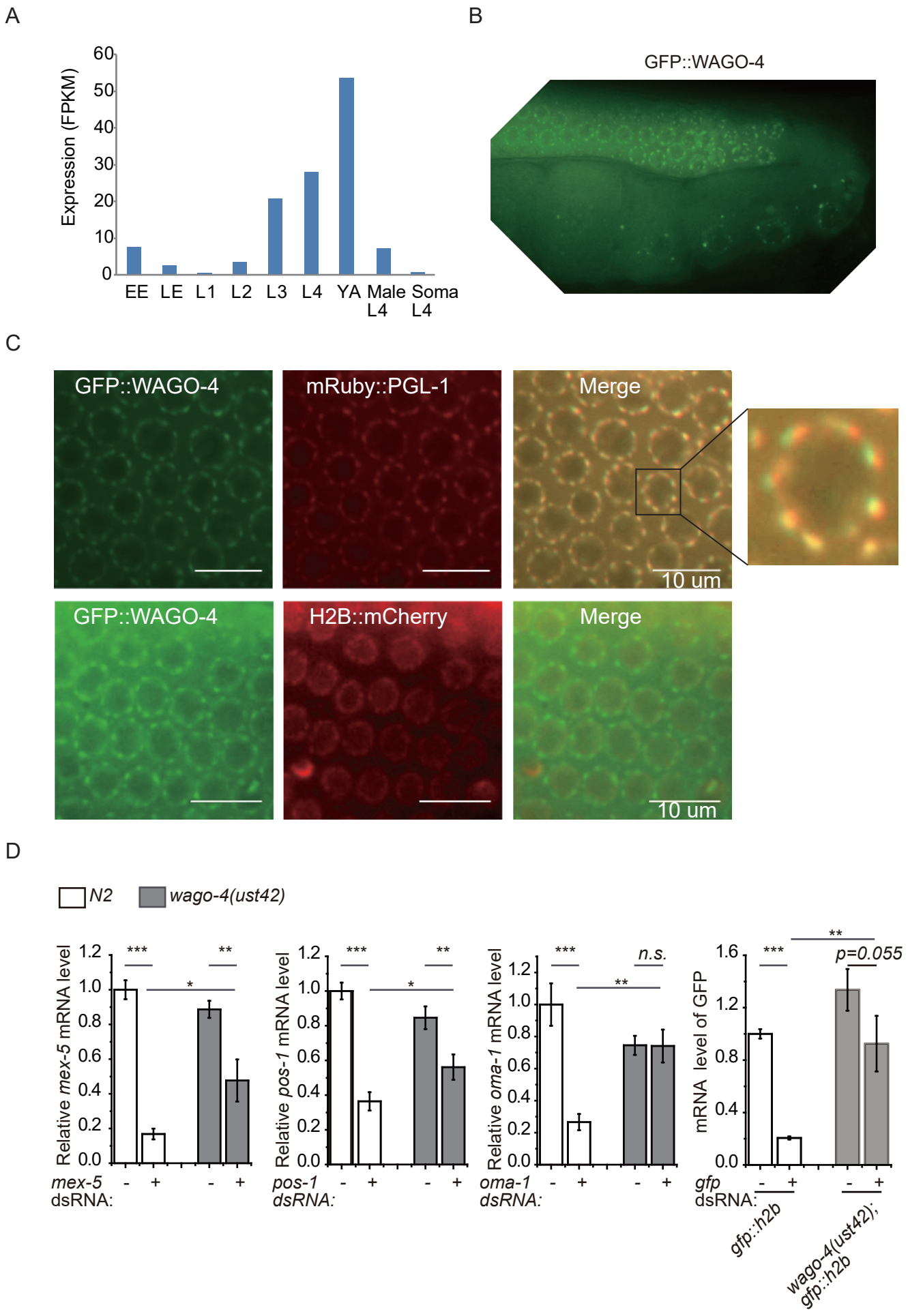
A
Expression (FPKM)
60
50
40
30
20
10
0
EE
LE
L1
L2
L3
L4
YA
Male L4
Soma L4
B
GFP::WAGO-4
C
GFP::WAGO-4
mRuby::PGL-1
Merge
10 um
GFP::WAGO-4
H2B::mCherry
Merge
10 um
D
N2
wago-4(ust42)
Relative mex-5 mRNA level
mex-5 dsRNA:
Relative pos-1 mRNA level
pos-1 dsRNA:
Relative oma-1 mRNA level
oma-1 dsRNA:
n.s.
mRNA level of GFP
p=0.055
gfp dsRNA:
gfp::h2b
wago-4(ust42); gfp::h2b

Figure 3

A

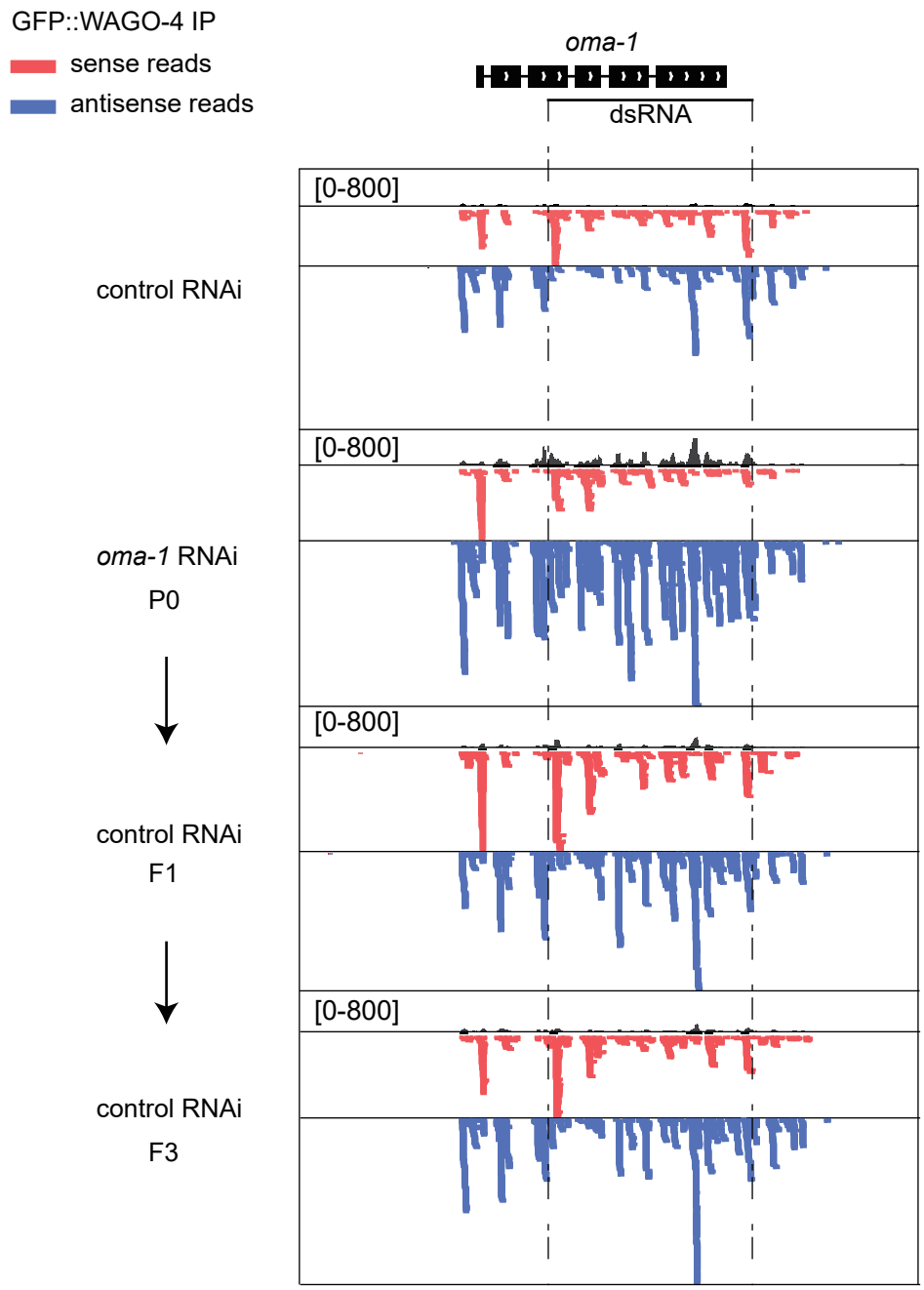
GFP::WAGO-4 IP
sense reads
antisense reads
oma-1
dsRNA
[0-800]
control RNAi
[0-800]
oma-1 RNAi
P0
[0-800]
control RNAi
F1
[0-800]
control RNAi
F3

B

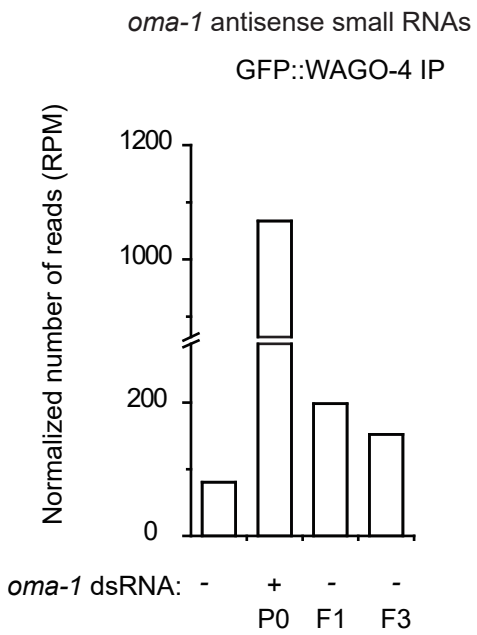
oma-1 antisense small RNAs
GFP::WAGO-4 IP
Normalized number of reads (RPM)
1200
1000
200
0
oma-1 dsRNA: - + - -
P0 F1 F3

C

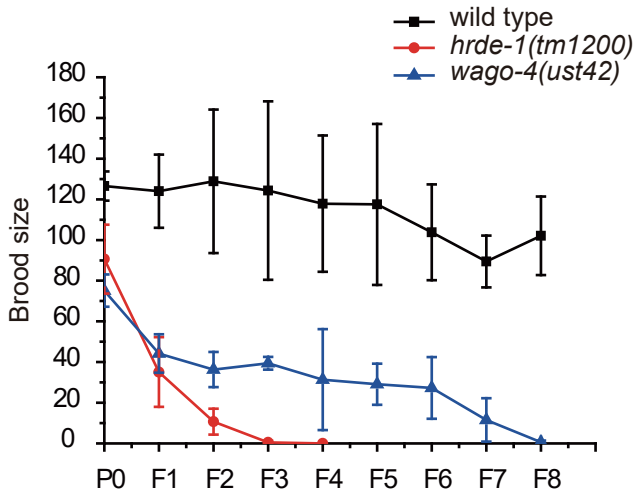
wild type
hrde-1(tm1200)
wago-4(ust42)
Brood size
180
160
140
120
100
80
60
40
20
0
P0 F1 F2 F3 F4 F5 F6 F7 F8

Figure 4

A

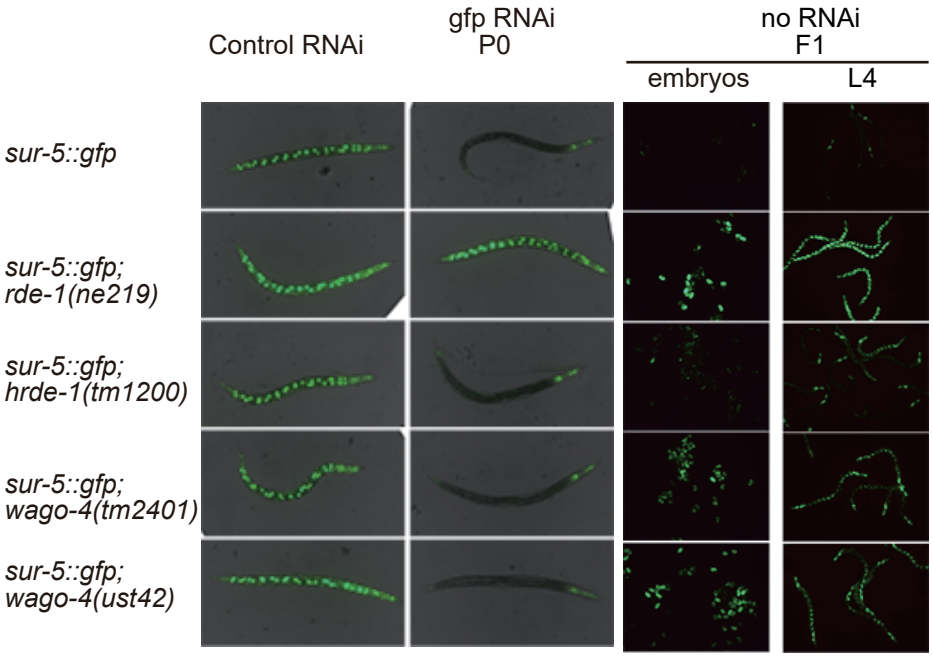
Control RNAi
gfp RNAi
P0
no RNAi
F1
embryos
L4
sur-5::gfp
sur-5::gfp;
rde-1(ne219)
sur-5::gfp;
hrde-1(tm1200)
sur-5::gfp;
wago-4(tm2401)
sur-5::gfp;
wago-4(ust42)

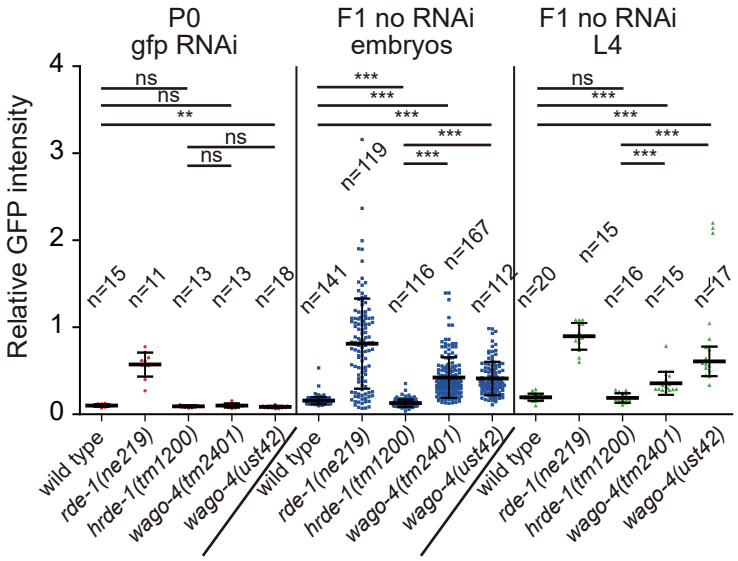
P0
gfp RNAi
F1 no RNAi
embryos
F1 no RNAi
L4
Relative GFP intensity
0
1
2
3
4
ns
ns
**
ns
ns
***
***
***
***
***
***
***
***
***
n=15
n=11
n=13
n=13
n=18
n=141
n=119
n=116
n=167
n=112
n=20
n=15
n=16
n=15
n=17
wild type
rde-1(ne219)
hrde-1(tm1200)
wago-4(tm2401)
wago-4(ust42)

B

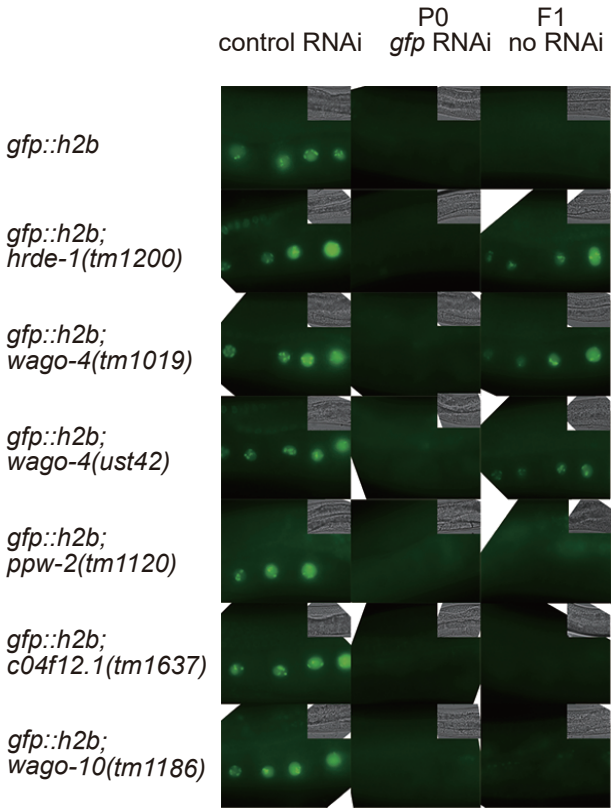
control RNAi
P0
gfp RNAi
F1
no RNAi
gfp::h2b
gfp::h2b;
hrde-1(tm1200)
gfp::h2b;
wago-4(tm1019)
gfp::h2b;
wago-4(ust42)
gfp::h2b;
ppw-2(tm1120)
gfp::h2b;
c04f12.1(tm1637)
gfp::h2b;
wago-10(tm1186)

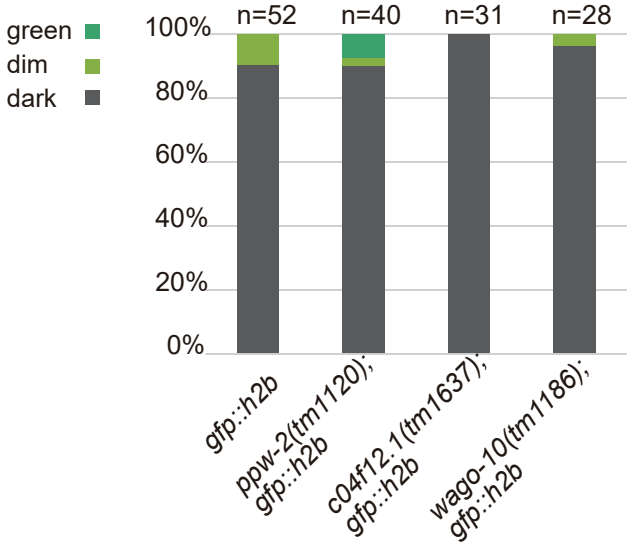
green
dim
dark
100%
80%
60%
40%
20%
0%
n=52
n=40
n=31
n=28
gfp::h2b
ppw-2(tm1120);
gfp::h2b
c04f12.1(tm1637);
gfp::h2b
wago-10(tm1186);
gfp::h2b

Figure 5

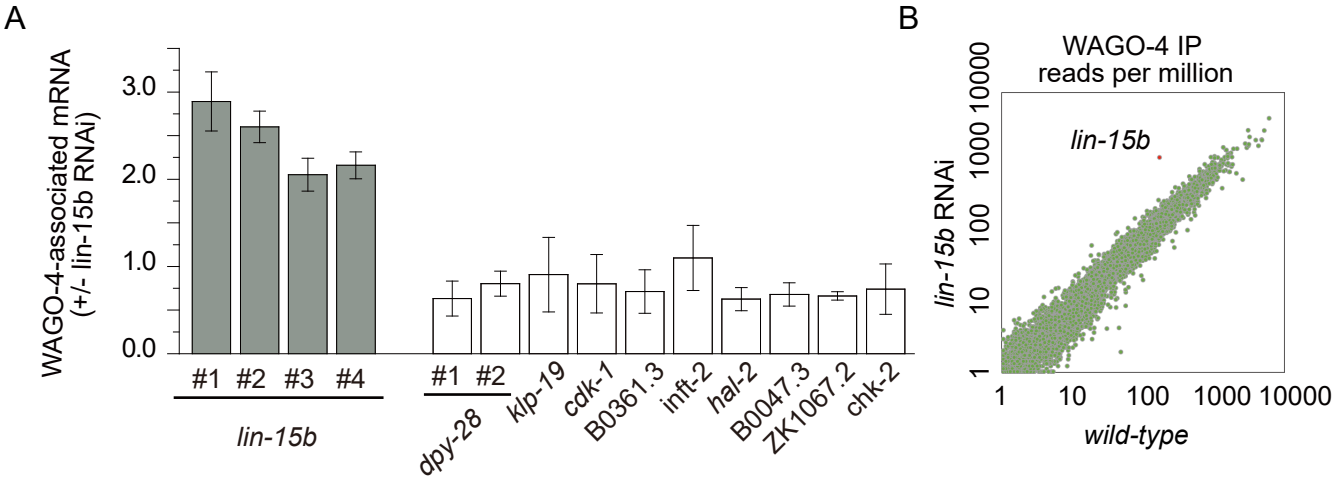
A
WAGO-4-associated mRNA
(+/- lin-15b RNAi)
3.0
2.0
1.0
0.0
#1 #2 #3 #4
lin-15b
#1 #2
dpy-28
klp-19
cdk-1
B0361.3
inft-2
hal-2
B0047.3
ZK1067.2
chk-2
B
WAGO-4 IP
reads per million
lin-15b
lin-15b RNAi
wild-type
1
10
100
1000
10000

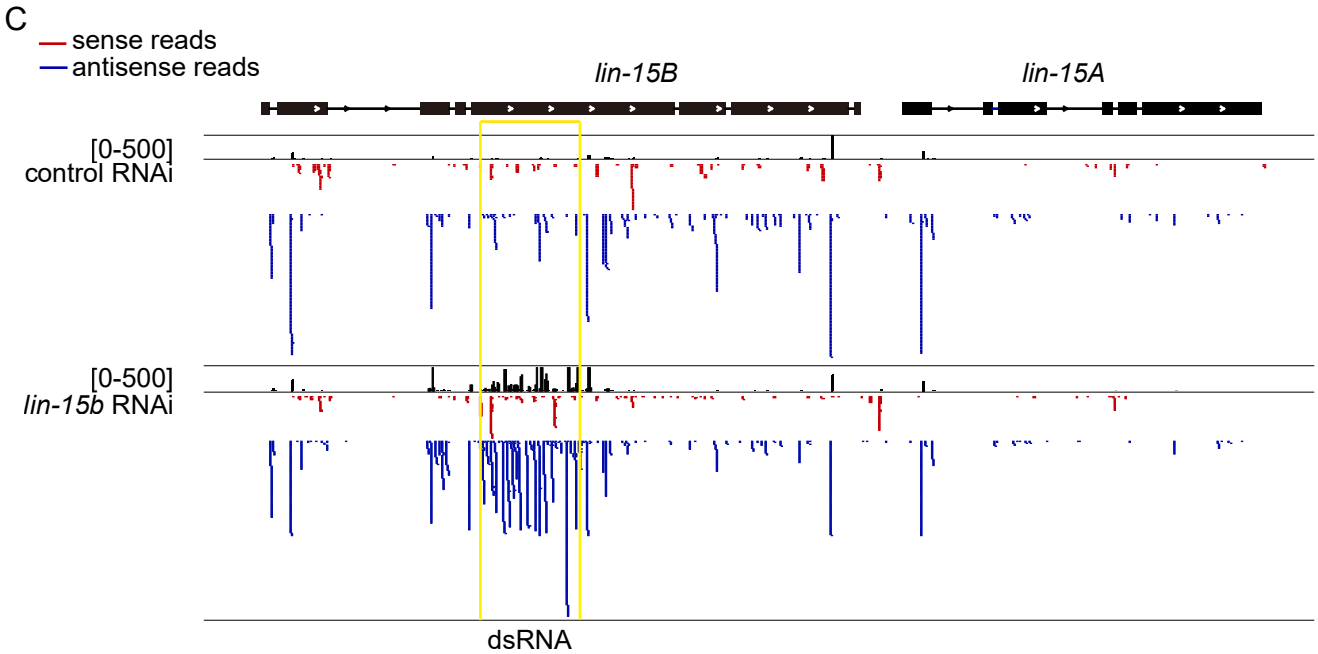
C
sense reads
antisense reads
lin-15B
lin-15A
[0-500]
control RNAi
[0-500]
lin-15b RNAi
dsRNA

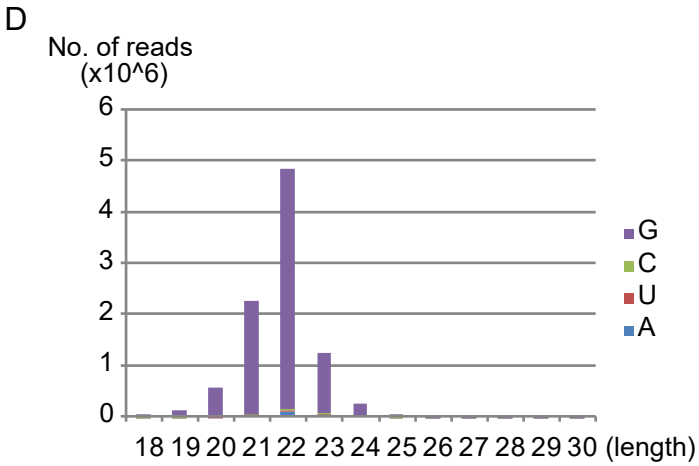
D
No. of reads
(x10^6)
6
5
4
3
2
1
0
G
C
U
A
18 19 20 21 22 23 24 25 26 27 28 29 30 (length)

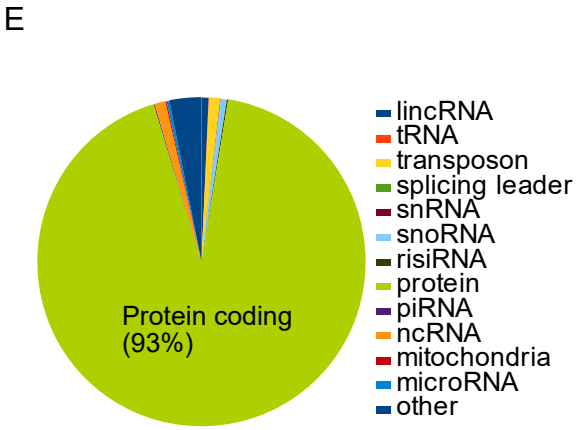
E
Protein coding
(93%)
lincRNA
tRNA
transposon
splicing leader
snRNA
snoRNA
risiRNA
protein
piRNA
ncRNA
mitochondria
microRNA
other

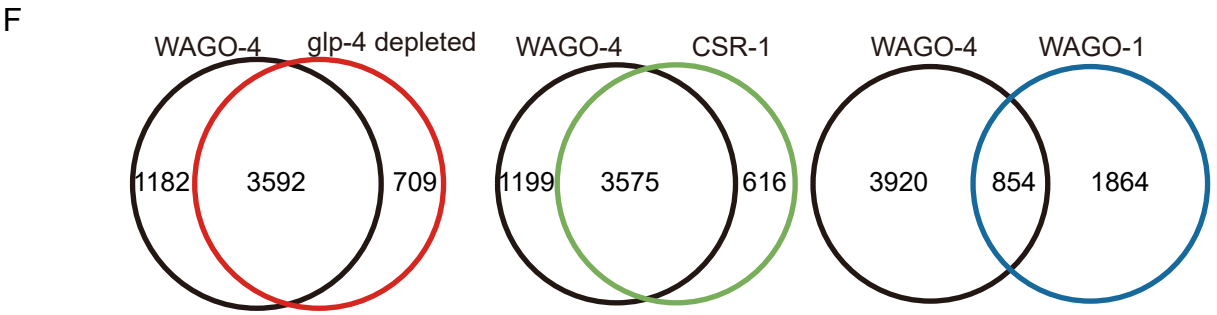
F
WAGO-4
glp-4 depleted
1182
3592
709
WAGO-4
CSR-1
1199
3575
616
WAGO-4
WAGO-1
3920
854
1864

Figure 6

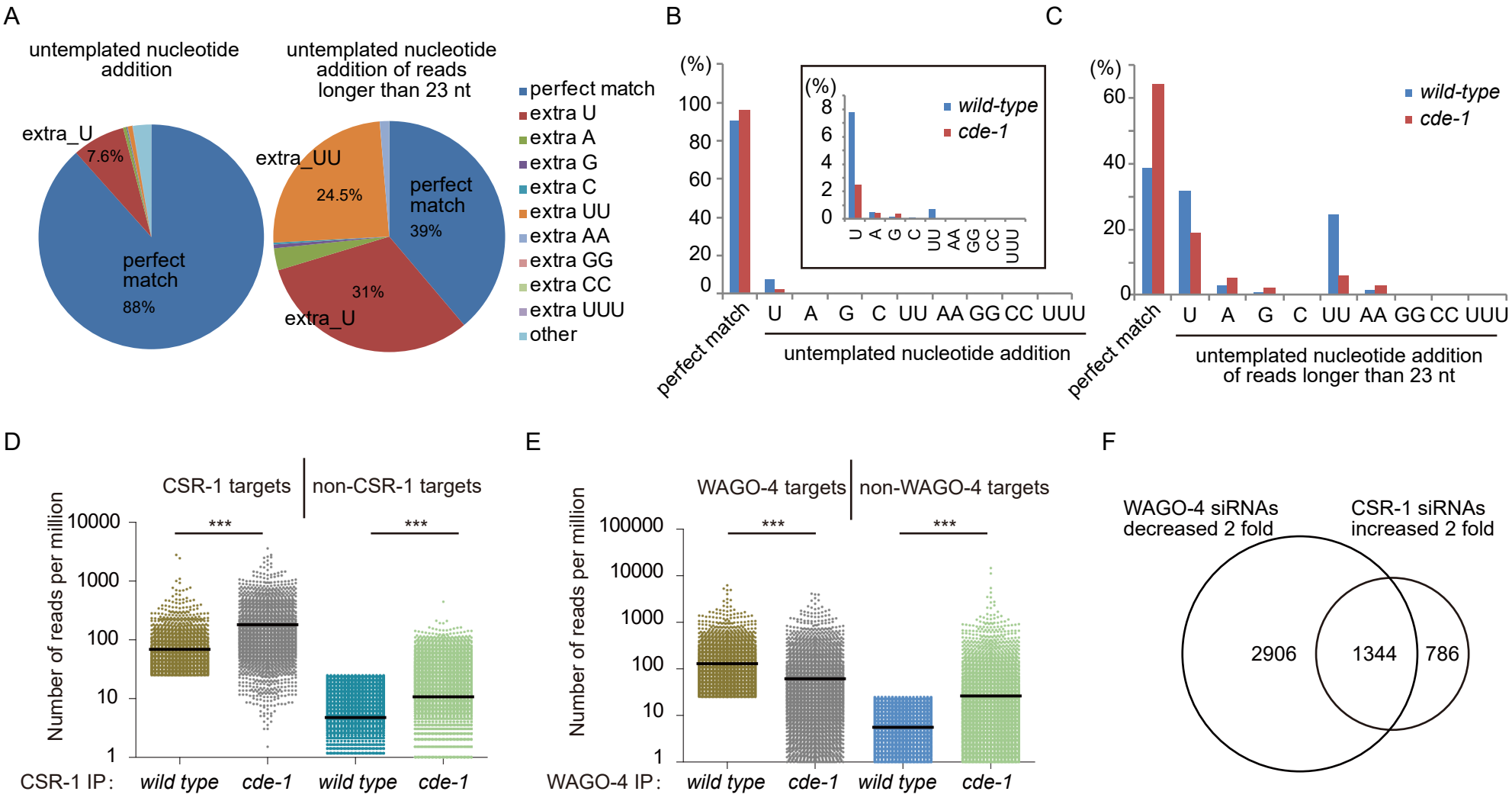
A
untemplated nucleotide addition
extra_U
7.6%
perfect match
88%
untemplated nucleotide addition of reads longer than 23 nt
extra_UU
24.5%
perfect match
39%
31%
extra_U
perfect match
extra U
extra A
extra G
extra C
extra UU
extra AA
extra GG
extra CC
extra UUU
other
B
(%)
100
80
60
40
20
0
wild-type
cde-1
U A G C UU AA GG CC UUU
perfect match
untemplated nucleotide addition
C
(%)
60
40
20
0
wild-type
cde-1
U A G C UU AA GG CC UUU
perfect match
untemplated nucleotide addition of reads longer than 23 nt
D
CSR-1 targets
non-CSR-1 targets
Number of reads per million
10000
1000
100
10
1
***
***
CSR-1 IP:
wild type
cde-1
wild type
cde-1
E
WAGO-4 targets
non-WAGO-4 targets
Number of reads per million
100000
10000
1000
100
10
1
***
***
WAGO-4 IP:
wild type
cde-1
wild type
cde-1
F
WAGO-4 siRNAs decreased 2 fold
CSR-1 siRNAs increased 2 fold
2906
1344
786

Figure 7

A

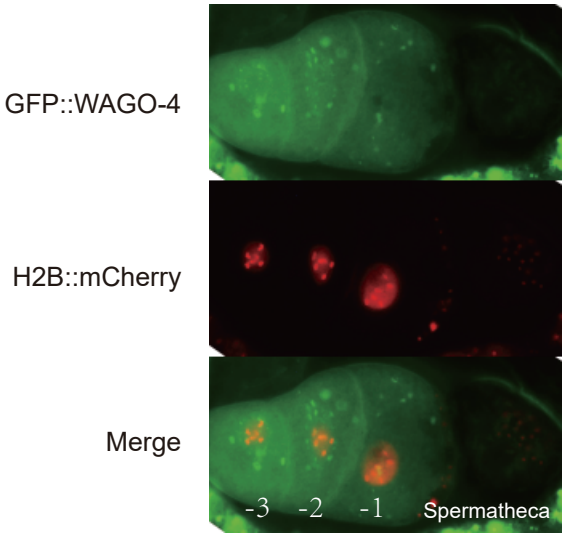

B

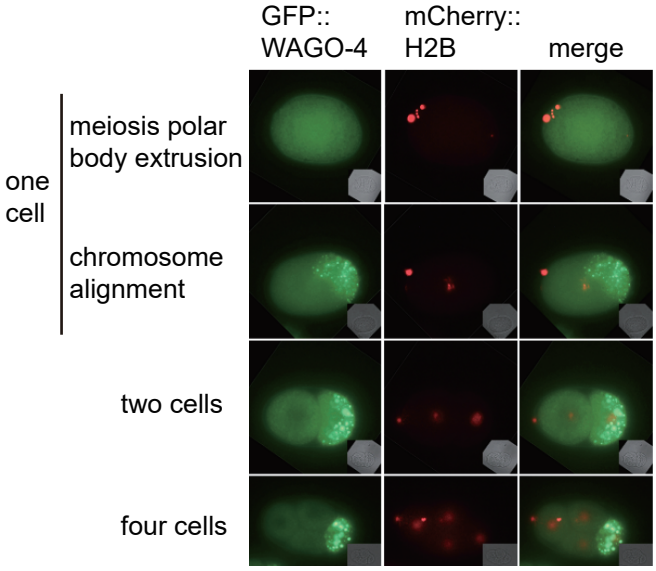

C

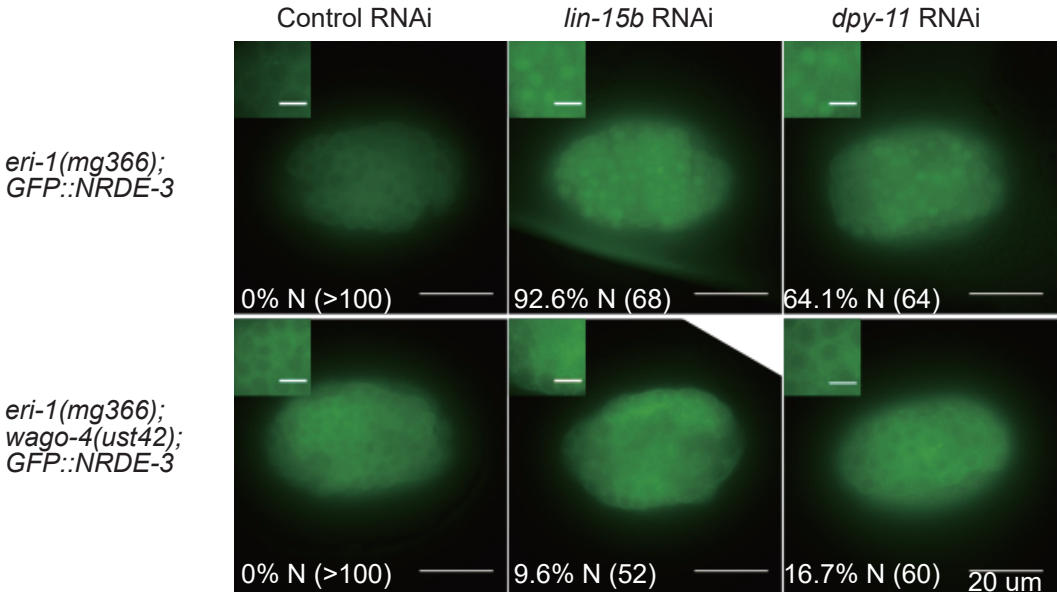
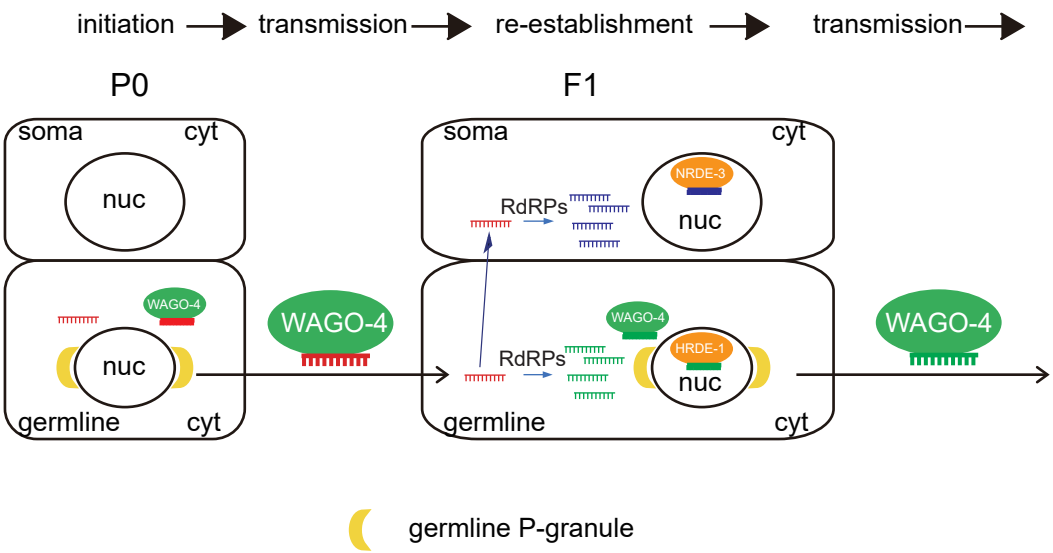
D